**LA-UR**-93-0048



Los Alamos National Laboratory is operated by the University of California for the United States Department of Energy under contract W-7405-ENG-36

LA-UR--93-0048

DE93 007352

TITLE THE NHMFL 60 TESLA, 100 MILLISECOND MAGNET



AUTHOR(S) Heinrich J. Boenig
Laurence J. Campbell
Dwight G. Rickel
John D. Rogers
Josef B. Schillig
James R. Sims
Paul Pernambuco-Wise

SUBMITTED TO 60 Tesla Design Review, Taos, NM, November 12-13, 1992

## DISCLAIMER





Los Alamos Los Alamos National Laboratory
Los Alamos, New Mexico 87545

November 9, 1992

# THE NHMFL 60 TESLA, 100 MS PULSED MAGNET

H. J. Boenig[a], L. J. Campbell[a], D. G. Rickel[a], J. D. Rogers[a], J. B. Schillig[a], J. R. Sims[a], P. Pernambuco-Wise[b], H. J. Schneider-Muntau[b]

[a)]National High Magnetic Field Laboratory,
Los Alamos National Laboratory, MS-E536, Los Alamos, NM 87545
[b)]National High Magnetic Field Laboratory,
Florida State University,1800 East Paul Dirac Drive, Tallahassee, FL 32306

## 1. INTRODUCTION

Among the new facilities to be offered by the National Science Foundation through the National High Magnetic Field Laboratory (NHMFL) are pulsed fields that can only be achieved at a national user facility by virtue of their strength, duration, and volume. In particular, a 44 mm bore pulsed magnet giving a 60 tesla field for 100 ms is in the final design stage. This magnet will be powered by a 1.4 GW motor-generator at Los Alamos and is an important step toward proving design principles that will be needed for the higher field quasi-stationary pulsed magnets that this power source is capable of driving.

The requirements for the magnet are

- — produce a 60T flat-top pulse for 100 ms;
- — have a recycle time of approximately 1 hour;
- — provide a 77K bore of 44 mm;
- — achieve field homogeneity of $10^{-3}$ or better in 10 mm sphere;
- — be robust and reliable, with a lifetime of 10 years or 10,000 pulses for the outer coils and a lifetime exceeding 1000 pulses for the inner coils;
- — permit higher field upgrades as better conductors or reinforcements become available;
- — be operational by early 1995.

These requirements lead to a poly-coil design consisting of several mechanically independent and spatially separated coils with external reinforcing shells. Among the advantages:

- —The reinforcement shell can be customized for each coil as needed to contain stress. This applies to both the hoop and axial stresses.
- —Different conductors can be used in different regions.
- —Independent power supplies can achieve fast rise times at lower voltage.
- —Coils can be individually sized for efficiency without sacrificing homogeneity.
- —Faster cooling occurs with separated coils.

—Individual coils are easily replaced to repair damage or install upgrades. (A possible upgrade path using a stronger conductor would be to substitute conductor turns for reinforcement thickness in one or more inner coils.)

—Conductive reinforcing shells can absorb energy from fast field transients caused by faults.

—Failure may be confined to a small number of coils.

A disadvantage to the poly-coil approach is the loss of packing fraction and the consequent need for greater power. However, the NHMFL motor-generator removes available power as a design constraint and cost attention is devoted more to power control and conversion.

To permit timely delivery of the magnet, it was decided to design with conductor and reinforcement materials now commercially available. Tests by NHMFL have confirmed that GlidCop-60 and GlidCop-15, dispersion strengthened copper alloys manufactured by SCM Metal Products, Inc., are adequate conductors for the 60T magnet.

## 2. MECHANICAL DESIGN AND STRESSES

The design evolved by manually iterating test solutions based on both discrete and averaged mechanical properties of the conductor-insulator coils in contact with reinforcing shells. A more automated iteration method was not attempted because of the difficulty of realistically including discrete and often unquantifiable design considerations related to fabrication, voltage-current, and thermal constraints.

For the most part, the design method follow that used by Lontai and Marston [1] to design the McGill University 10T magnet. This essentially treats the coil and shell as separate continua in a linear background field distribution at the midplane and solves the elastic equations for the hoop stress in the presence of a uniformly distributed Lorentz force in the coil. Only the midplane is treated. Other programs calculate the axial forces which can be included to yield the effective von Mises stress at the midplane. The effect of axial forces was included using results of Markiewicz *et al* [2] which show how axial stress is efficiently transferred to the reinforcing shell, especially in thin coils.

Drawings of the magnet in perspective and cross-section are shown in Figs. 1 and 2. The total conductor mass is 5293 kg and the total reinforcing shell mass is 1527 kg.

The mounting assembly makes provision for aligning the magnetic centers of the 8 coils. The final alignment occurs automatically as the coils are energized and seek their position of lowest energy by moving against leaf springs in the mount. This assembly is shown in Fig. 3 and the assembly in the LN dewar is shown in Fig. 4.

Table 1 contains the mechanical specifications.of the 8 coils. Note that the estimated packing fraction realistically takes account of the inevitable winding error.

In studying the stress it was found that thermal loading of some of the windings contributed to stress containment. That is, pre-stressing the reinforcement shell by thermal expansion of the coil (or thermal contraction of the shell during cool-down) effectively loads the coil against the shell and results in smaller coil magnetic stress during the pulse. The problem is illustrated in Fig. 5 which shows the midplane hoop elastic stress without thermal pre-stressing. Note that the stress of the innermost layer of coil 2 (denoted by "E") lies at or above the elastic limit (denoted by the horizontal line labeled E on the right). At the same time the stress in the shell of coil 2 is far below its yield limit (denoted by the horizontal line labeled S on the right). The effect of thermal pre-stressing is to raise the stress in the shell and lower it in the coil. The requirement for robustness has driven the stress design to stay below yield for maximum field pulses, although during the training period some excursions to yield may occur, again for the purpose of obtaining pre-stress.

The midplane radial displacements occurring in the absence of pre-stressing are shown in Fig 6 as cm and in Fig. 7 as percentages. These displacements overestimate the displacement with pre-stress. Even so, the elongation is less than 0.5% for most coils.

The total axial stress on the midplane of each layer are shown in Fig. 8. This is the Lorentz axial stress that takes no account of sharing the stress with the shell or other layers through shear. Likewise, Fig. 9 gives the axial forces per turn for the inner coils where it is strongest.

When account is taken of the thermal pre-stressing and the transfer of axial stress (in the manner described by Markiewicz *et al* [2]) the resulting stresses lie within yield, as listed in Table 2 and shown in Figs. 10 and 11 for interface pressure and thermal stress and the winding and shell stresses, respectively.

## 3. MATERIALS

Realization of high field non-destructive magnets is material limited: conductors of high strength, high conductivity, high specific heat, and good elongation; reinforcement material of high strength at 77K and superior fatigue strength; insulation of low compressibility, high viscosity and high thermal conductivity. The commercial materials chosen for the magnet are as follows.

Conductor: (Al-15 is used for coil 1, AL-60 for coils 2 through 8.)

| | GlidCop AL-15 | GlidCop AL-60 |
|---|---|---|
| yield strength (0.2%) @ 77 K | 594 MPa | 745 MPa |
| ultimate strength @ 77 K | 684 MPa | 856 MPa |
| Young's modulus | 139 GPa | 143 GPa |
| elongation @ RT | 12.5 % | 9.2 % |
| elect. resistance ratio (77 K/RT) | 4.84 | 3.98 |
| %IACS conductivity @ RT | 88.7 | 79.5 |
| total thermal contraction, RT to 77 K | 0.278 % | 0.190 % |

Reinforcement:

| | Nitronic 40 (annealed) |
|---|---|
| yield strength (0.2%) @ 77 K | 1.0 GPa |
| ultimate strength @ 77 K | 1.4 GPa |
| fatigue strength (1000 cycles) @ 77 K | 1. GPa |
| Young's modulus @ 77 K | 186 GPa |
| elongation @ 77 K | 23 % |
| elect. resistivity @ 77 K | 63 micro-ohm-cm |
| thermal conductivity @ 77 K | 7 W/mK |
| total thermal contraction, RT to 77 K | 0.259 % |

Insulation:

| | CTD-101G | CTD-101 w/ 50% g |
|---|---|---|
| compression strength @ 77 K | 560 MPa | 1.25 GPa |
| compression modulus @ 77 K | 17.7 GPa | |
| shear strength @ 77 K | 170 MPa | 200 MPa |
| shear modulus @ 77 K | 8.2 GPa | 9.1 GPa |
| thermal conductivity @ 77 K | 10-20 W/mK | |
| total thermal contraction, RT to 77 K | 0.4% | |
| viscosity @ 110 °C | 2,000 cP | |

The CTD-101G resin is 67% alumina by weight and has a remarkably high thermal conductivity. This makes it possible to cool coil 8 in one hour. The characteristics for CTD-101, which can be used for the thin coils, 1 through 7, refer to the impregnated composite of resin and 50% S-2 fiberglass. The conductor will be half-lapped with fiberglass and Kapton tape before being wound on the mandrel. The coils will then be potted in the usual manner, with the reinforcing shell used as part of the impregnation mold for some of the coils.

# 4. ELECTRICAL BEHAVIOR

## 4.1 Results and Parameters

The lengths of the inner windings were chosen to reach 95% field efficiency (compared to an infinitely long coil) and to remain within homogeneity limits. This is illustrated in Fig. 12. The 1-cm homogeneity is predicted to be $1.3\ 10^{-4}$. Contours of the field strength are shown in Fig. 13. These fields are used to predict the force on current leads to the coils. The midplane magnetic profile is given in Fig. 14.

Table 3 lists the electrical parameters that give the above fields. Note that the identical currents in coils 1 through 7 do not imply a common power supply.

## 4.2 Electrical Circuit

The design of the power supply for the 60 T magnet is a compromise between many parameters, such as coil stress and heating, modularity, upgrade capability and cost. The inner coils are designed for a shorter current pulse than the outer coil. Therefore, the coils are partitioned electrically into several groups. Although the seven inner coils have the same peak current, they must be partitioned further into two groups to avoid overheating the inner coils: the inner group comprising coils 1, 2, and 3 and the intermediate group of coils 4, 5, 6 and 7. Coil 8 is treated independently. Because of the strong influence of the mutual coupling, it was decided to keep the current in the outer groups nearly constant while the current in the inner group ramps up (Fig. 15). If the current in the inner coil group is ramped up while the outer groups are still ramping, a considerably higher voltage must be applied to maintain the ramp rate in the outer coils.

Three power supplies are used for the three groups: coils 1-3, 4-7, and 8, respectively. Table 4 gives the peak current, $I_p$, voltage at the peak current, V, and the peak power requirement, P. The values of Table 4 are taken from simulation results. Coil 3 was included in the inner coil group to have enough inductance in the circuit to obtain an acceptable ripple value during the 60T, 100 ms flat top.

Given the peak current values and the required voltage values at peak current, the no-load voltage of the each supply can be determined. Assuming a 16% voltage drop between no-load and full-load voltage, the following no-load voltage, $V_0$, is obtained:

| | |
|---|---|
| Supply 1 | $V_0 = 1.2$ kV |
| Supply 2 | $V_0 = 8.0$ kV |
| Supply 3 | $V_0 = 12.0$ kV |

A 16% voltage drop for pulsed converters is a reasonable assumption. Supplies with such a voltage drop have been built for pulsed fusion experiments. A power supply with a no-load voltage in the range of 10 kV must be built up from several modules, which have no-load voltages in the range of 3 to 4 kV. Let us propose the higher voltage 4 kV design. The outer coil supply will need three modules, connected in series. The intermediate coils will need two modules connected in series. Each module is a 12 pulse unit, consisting of two series-connected 6 pulse units. Two 12 pulse modules can be arranged as one 24 pulse unit. However, because of the large inductance, the additional circuit complexity does not justify the small improvement in the ripple. Fig. 16 (in the text) shows the supply module arrangement for the outer coil and the intermediate coils.

A module consists of a 24 kV circuit breaker, a three winding transformer, two series connected 6 pulse bridges and two 'thyristorised' crowbar paths. Each bridge has an output voltage of 2 kV and an input voltage of 1.5 kV. While the voltage rating of the two major supplies can be satisfied with identical modules, the current rating is different, because the current pulse length is different. The supply for the outer coil must be designed for a trapezoidal current with a 1.6 s rise and fall time and a 0.8 s flat top-time. Assuming a flat-top current

**Table 4.** Power Supply Parameters

| | $I_p$ | V | P |
|---|---|---|---|
| Supply 1 (coil 1, 2, 3) | 18.64 kA | 10.0 kV | 18.64 MW |
| Supply 2 (coil 4, 5, 6, 7) | 18.64 kA | 6.6 kV | 123.00 MW |
| Supply 3 (coil 8) | 16.52 kA | 10.0 kV | 165.00 MW |

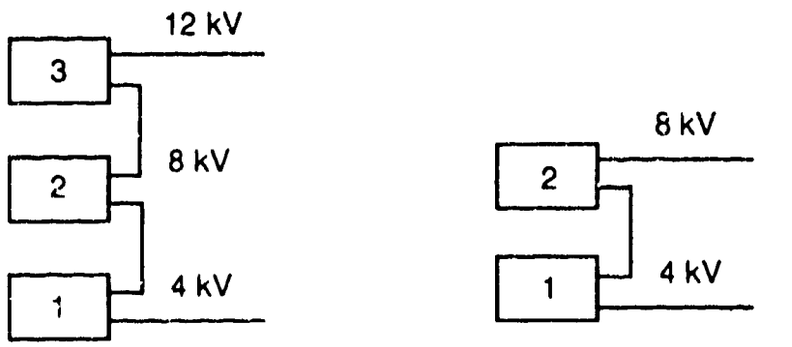


**Figure 16.** Power supply module arrangement for coil groups.

of 17 kA, the supply current must be dimensioned for an $I^2t$ rating of $540 \cdot 10^6$

$A^2S$. An equivalent rectangular current with an amplitude of 17 kA and a pulse length of 2 s (1.866 s, more precisely) has the same heating effect.

The supply for the intermediate coils has a rise and decay time of about 0.3 s, a flat-top time of 0.225 s and a flat-top current of 18.6 kA. The equivalent rectangular pulse current with a 17 kA amplitude has a pulse length of 0.4s. If minimum cost is the only determining factor for purchasing the power supplies, NHMFL will have two different types of power supply modules for the 60T magnet. Considering the fact that a facility is being built which should supply power for magnets above 60T with increased power requirements the preferred choice is to buy 12 pulse, 4 kV, 20 kA, 2 s pulse length modules. These modules can be connected in parallel and series to accommodate different requirements.

The inner coil group will be supplied by an existing 12 pulse power supply. Each power supply should be equipped with a free wheeling path, made of thyristors.

### 4.3 Electrical Ripple

Power supplies generate voltage ripple when the bridge converters are phased back, resulting in a lower average output voltage. At the beginning of the flat top the average coil voltages are the smallest, resulting in the highest ripple voltages. If the simplest converter control strategy is used to achieve the reduction in average voltage, the ripple current can be calculated to be $2.5 \cdot 10^{-3}$, $0.3\ 10^{-3}$ and $5.5\ 10^{-3}$ for the field produced by the inner, intermediate and outer coil group respectively. Table 5 gives the assumption for the ripple calculation with $V_o$ the supply no-load voltage, V the average voltage at the beginning of the flat-top, $V_{pp12}$ and $I_{pp12}$ the peak to peak $12^{th}$ harmonic voltage and current, L the inductance of the coil group and R the ratio of $I_{pp12}$ to the flat-top current, Imax. All the values are approximated. As expected, the inner coil group doesn't have enough inductance to smooth out the current. Some advanced converter control for the inner coil group supply can reduce the ripple to $5 \cdot 10^{-4}$.

**Table 5.** Ripple Calculation

| | $V_o$ | V | $V_{pp12}$ | L | $I_{pp12}$ | $I_{max}$ | R |
|---|---|---|---|---|---|---|---|
| Supply 1 | 1.2 kV | 0.45 kV | 0.7 kV | 5.00 mH | 41 A | 18.64 kA | $2.5 \cdot 10^{-3}$ |
| Supply 2 | 8.0 kV | 4.70 kV | 3.0 kV | 0.15 H | 6 A | 18.64 kA | $3.0 \cdot 10^{-4}$ |
| Supply 3 | 12.0 kV | 3.80 kV | 8.0 kV | 0.80 H | 3 A | 16.50 kA | $1.7 \cdot 10^{-4}$ |

## 5. THERMAL BEHAVIOR

There are two aspects to the thermal behavior, one critical and the other convenient.

The critical thermal behavior is the final coil temperature, because the epoxy insulation degrades at temperatures modestly above room temperature. In this design, no coil reaches such temperatures. Another issue is the heating of the metallic shells due to induced currents during field changes. The predicted temperature rise and the energy deposited in the steel shells are shown in Fig. 17. The winding and shell temperatures after a pulse are summarized in Fig. 18.

The convenient side of thermal behavior is the cool-down time of the magnet, because this fixes the maximum number of shots per day. Coil 8, being the thickest, determines the cool-down. Thanks to the high thermal conductivity of CTD-101G alumina-loaded resin the goal of one-hour cooling can be reached, as shown in Figs. 19, 20, and 21 for different starting temperatures, different thermal conductivities of the insulating resin, and different coil thicknesses, respectively.

## 6. MOTOR-GENERATOR

### 6.1 Background

Los Alamos National Laboratory' s "1430 MVA Generator Facility" is based on a motor-generator set which in it's current configuration is capable of producing high power pulses of up tc 1040 MVA of peak power and up to 600 MJ of energy. This same set and the facility could, given the need and the funds, be upgraded to provide pulses of up to about 2000 MVA and 2000 MJ.

Besides the regular, high power, long pulse applications of the motor-generator there are other possible uses, such as:

3 - Phase loads. High current, low power, long and very long pulses. (As installed, up to 25 kA; maximum, up to about 50 kA)

2 - Phase loads. Very short pulses, as long as one cycle. (As installed, up to 840 MVA apparent power; maximum, up to about 1680 MVA)

"Short circuit loads" with hardly any voltage, current controlled. (As installed, up to 25 kA; maximum, up to 50 kA)

All of the above applications would require modifications to the existing facility configuration.

## 6.2 Capabilities of the Generator Facility

The list below gives some of the basic rated data of the motor-generator.

| | | |
|---|---|---|
| Rated power | 1430 | MVA |
| Rated voltage | 24 | kV |
| Rated current | 34.4 | kA |
| Rated field voltage | 670 | V |
| Rated field current | 8100 | A |
| Rated frequency | 60 | Hz |
| Rated speed | 1800 | rpm |

The following table summarizes some of the capabilities and limitations of the facility for the long pulse regime. This data is valid for the facility as it is configured to date.

| | | |
|---|---|---|
| Pulse power range | 0 - 1040 | MVA |
| Pulse voltage range | 0 - 24 | kV |
| Pulse current range | 0 - 25 | kA |
| Pulse speed range | 1260 - 1800 | rpm |
| Stored energy @ 1800 rpm | 1260 | MJ |
| Extractable energy (1800 rpm → 1260 rpm) | 600 | MJ |
| Full pulse repetition rate | 10 | /min |
| Maximum pulse duration @ 24 kV | 10 | s |
| Maximum pulse duration @ 25 kA | 2 | s |
| Maximum effective current averaged over a 10 minute period | 1.8 | kA |
| Maximum field voltage | 1025 | V |
| Maximum field current | 5130 | A |
| | | |
| Run up time (9 rpm → 1800 rpm) | 15 | min |
| Run up time between full pulses (1260 rpm → 1800 rpm) | 7 | min |
| Run down time (1800 rpm → 9 rpm) | 6 | min |
| | | |
| Coast down time (1800 rpm → 9 rpm) | 38 | min |
| | | |
| Fatigue life: Start / Stop (9 rpm → 1800 rpm → 9 rpm) | 1700 | Cycles |
| Full pulses (1800 rpm → 1260 rpm → 1800 rpm) | $10^5$ | Cycles |

The above tables show that the facility can easily cover the needs of the NHMFL projects to be realized in the near future (i.e. 60 T magnet system).

## 6.3 Possible Upgrades

The facility can be upgraded in several different ways, depending on the needs and funds available.

**Increase of the stored and extractable energy**

With a flywheel the stored energy at 1800 rpm could be increased from 1260 MJ to a maximum of about 4000 MJ. This would increase the extractable energy from 600 MJ to about 2000 MJ. Together with an increase of the pulse power output this will most likely satisfy all possible needs of the magnet facility even for the distant future.

Sharp and at the same time high magnitude load transitions will significantly shorten the fatigue life of the shaft train in this configuration (Power transients of about 1500 MW in 20 ms reduce the fatigue life to about 800 full pulse cycles).

The run up times upon start up and re-acceleration between pulses would be about three to four times longer. The same is true for the run down and coast down times.

The machine set and the foundation are already designed to accommodate a future flywheel. Space for the necessary auxiliary equipment is also reserved. The control system is designed to accommodate the additional control and protection tasks.

**Increase of the power output**

The pulse power output is at the time limited by the following elements:

— current limiting and interrupting device;
— load breaker;
— excitation transformer.

The current limiting and interrupting device, currently under procurement, will be one of highest rated devices of it's kind worldwide (24 kV, 25 kA, 2 s, with a trigger level of 35 to 40 kA momentary current). The use of this element greatly reduces the costs for the 24 kV bus by making it possible to use standard industrial bus designs, high voltage breakers and related equipment. It also limits drastically the extent of damages in case of faults on the primary side of the power converter transformers.

Our experiences with this device, future developments of this product and more elaborate schemes will certainly make even higher ratings possible .

## 7. SCHEDULE AND COST ESTIMATE

Table 6 lists estimates of sub-task completion dates and times and some costs.

---

This work was supported by NHMFL and the National Science Foundation under cooperative agreement No. DMR-9016241.

---

## References

1. L. M. Lontai and P. G. Marston, "A 100 Kilogauss Quasi-Continuous Cryogenic Solenoid - Part I," *Proc. Intern. Symp. Magnet Technology*, 723, Stanford, 1965.
2. W. D. Markiewicz, S. R. Voleti, N. Chandra, and F. S. Murray, "Transverse Stress on Nb3Sn Conductors in High Field NMR Magnets," Proceedings of the Applied Superconductivity Conf., Chicago, 1992.

## Tables



## Figures

MECHANICAL INFORMATION

| Winding | one | two | three | four | five | six | seven | eight |
|---|---|---|---|---|---|---|---|---|
| Alpha (Winding OD/Winding ID) | 1.53 | 1.64 | 1.33 | 1.20 | 1.07 | 1.06 | 1.05 | 1.68 |
| Beta (Winding Height/Winding ID) | 4.26 | 4.19 | 3.55 | 3.33 | 2.28 | 1.92 | 1.65 | 1.45 |
| Winding ID (cm) | 4.75 | 9.06 | 18.3 | 30 | 43.8 | 52.16 | 60.52 | 69.08 |
| Winding OD (cm) | 7.26 | 14.9 | 24.4 | 36.1 | 46.86 | 55.22 | 63.58 | 116.32 |
| Winding Radial Thickness (cm) | 1.26 | 2.92 | 3.05 | 3.05 | 1.53 | 1.53 | 1.53 | 23.62 |
| Winding Average Radius (cm) | 3.00 | 5.99 | 10.68 | 16.53 | 22.67 | 26.85 | 31.03 | 46.35 |
| Winding Height (cm) | 20.25 | 38 | 65 | 100 | 100 | 100 | 100 | 100 |
| Reinforcing Shell OD (cm) | 8.46 | 17.7 | 29.4 | 43 | 51.36 | 59.72 | 68.28 | ---- |
| Reinforcing Shell Thickness (cm) | 0.6 | 1.4 | 2.5 | 3.45 | 2.25 | 2.25 | 2.35 | ---- |
| Reinforcing Shell Height (cm) | 25.3 | 41.0 | 70.1 | 106.0 | 106.0 | 106.0 | 106.0 | ---- |
| Reinforcing Shell Mass (kg) | 2.94 | 23.01 | 115.93 | 355.78 | 288.12 | 337.16 | 403.99 | ---- |
| Radial Winding Error per Layer (cm) | 0.07 | 0.07 | 0.07 | 0.07 | 0.07 | 0.07 | 0.07 | 0.09 |
| Axial Winding Error per Turn (cm) | 0.03 | 0.03 | 0.03 | 0.04 | 0.04 | 0.04 | 0.04 | 0.12 |
| Winding Packing Factor | 0.65 | 0.70 | 0.70 | 0.70 | 0.70 | 0.70 | 0.70 | 0.74 |
| Conductor Size Hght x Wdth (cm) | .78x.47 | .95x.57 | 1.0x.6 | 1.0x.6 | 1.0x.6 | 1.0x.6 | 1.0x.6 | 1.4x1.0 |
| Conductor Cross-Sect. Area (cm^2) | 0.3613 | 0.5362 | 0.5947 | 0.5947 | 0.5947 | 0.5947 | 0.5947 | 1.3947 |
| IR to Innermost Cu Surface (cm) | 2.41 | 4.58 | 9.20 | 15.05 | 21.95 | 26.13 | 30.31 | 34.59 |
| OR to Outermost Cu Surface (cm) | 3.58 | 7.40 | 12.15 | 18.00 | 23.38 | 27.56 | 31.74 | 58.11 |
| Turns per Layer | 23 | 36 | 59 | 90 | 90 | 90 | 90 | 63 |
| Layers | 2 | 4 | 4 | 4 | 2 | 2 | 2 | 20 |
| Turns (total) | 46 | 144 | 236 | 360 | 180 | 180 | 180 | 1260 |
| Conducer Length (m) | 8.7 | 54.2 | 158 | 374 | 256 | 304 | 351 | 3669 |
| Conductor Mass (kg) | 2.76 | 25.60 | 83 | 196 | 134 | 159 | 184 | 4509 |
| Conductor Alloy | AL-15 | AL-60 | AL-60 | AL-60 | AL-60 | AL-60 | AL-60 | AL-60 |
| Combined Winding & Shell Mass (kg) | 5.70 | 48.62 | 199 | 552 | 422 | 496 | 588 | 4509 |
| | | | | | | | | |
| Total Conductor Mass (kg) = | 5293 | | Conductor corner radii are 0.0787 cm, | | | | | |
| Total Reinforcing Shell Mass (kg) = | 1527 | | 0.3 cm wide annuli between windings 1 through 4, | | | | | |
| Total Metal Mass (kg) = | 6820 | | 0.4 cm wide annuli between windings 4 through 8. | | | | | |
| | | | Winding 1 lined with a 0.15 cm wall thickness | | | | | |
| | | | epoxy fiberglass laminate tube to protect winding. | | | | | |

Table 1.

STRESS INFORMATION

| Winding | one | two | three | four | five | six | seven | eight |
|---|---|---|---|---|---|---|---|---|
| Bo (T) | 60 | 54.9 | 46.44 | 38.363 | 30.356 | 26.516 | 22.801 | 19.218 |
| delta B (T) | 5.1 | 8.46 | 8.077 | 8.007 | 3.84 | 3.715 | 3.583 | 19.218 |
| Beta | 4.263 | 4.194 | 3.552 | 3.333 | 2.283 | 1.917 | 1.652 | 1.448 |
| Wndng ID (cm) | 4.75 | 9.06 | 18.3 | 30 | 43.8 | 52.16 | 60.52 | 69.08 |
| Wndng OD (cm) | 7.26 | 14.9 | 24.4 | 36.1 | 46.86 | 55.22 | 63.58 | 116.32 |
| delta r (cm) | 1.255 | 2.92 | 3.05 | 3.05 | 1.53 | 1.53 | 1.53 | 23.62 |
| r avg (cm) | 3.0025 | 5.99 | 10.675 | 16.525 | 22.665 | 26.845 | 31.025 | 46.35 |
| Length (cm) | 20.25 | 38 | 65 | 100 | 100 | 100 | 100 | 100 |
| OD Spprt (cm) | 8.46 | 17.7 | 29.4 | 43 | 51.36 | 59.72 | 68.28 | ---- |
| Spprt Thk (cm) | 0.6 | 1.4 | 2.5 | 3.45 | 2.25 | 2.25 | 2.35 | ---- |
| Packing Fctr | 0.654 | 0.696 | 0.708 | 0.702 | 0.7 | 0.7 | 0.7 | 0.744 |
| Cndctr Sz H x W (cm) | .78x.47 | .95x.57 | 1.0x.6 | 1.0x.6 | 1.0x.6 | 1.0x.6 | 1.0x.6 | 1.4x1.0 |
| Cndctr X-sect area (cm^2) | 0.3613 | 0.5362 | 0.5947 | 0.5947 | 0.5947 | 0.5947 | 0.5947 | 1.3947 |
| IR to Cu Surf (cm) | 2.4106 | 4.5808 | 9.2008 | 15.051 | 21.951 | 26.131 | 30.311 | 34.591 |
| OR to Cu Surf (cm) | 3.5792 | 7.3992 | 12.149 | 17.999 | 23.379 | 27.559 | 31.739 | 58.109 |
| Turns (total) | 46 | 144 | 236 | 360 | 180 | 180 | 180 | 1260 |
| Layers | 2 | 4 | 4 | 4 | 2 | 2 | 2 | 20 |
| Cndctr Length (m) | 8.678 | 54.196 | 158.29 | 373.79 | 256.33 | 303.61 | 350.88 | 3669.4 |
| j (kA/cm^2) | 51.6 | 34.76 | 31.34 | 31.34 | 31.34 | 31.34 | 31.34 | 11.85 |
| I (kA) | 18.64 | 18.64 | 18.64 | 18.64 | 18.64 | 18.64 | 18.64 | 16.52 |
| Peak I (kA) | 18.64 | 18.64 | 18.64 | 18.64 | 18.64 | 18.64 | 18.64 | 17.2* |
| Winding Temp I (K) | 97 | 92 | 87 | 155 | 155 | 155 | 155 | ---- |
| Winding Temp F (K) | 150 | 128 | 113 | 196 | 196 | 196 | 196 | ---- |
| Shell Flat Top Temp (K) | 77.3 | 78.1 | 79.6 | 81.3 | 82.5 | 83.3 | 83.2 | |
| Raw Wnd Axl Strs (MPa)I | 12 | 43 | 135 | 364 | 429 | 464 | 495 | 198* |
| Rw Wnd Axl Strs (MPa) Av | 12 | 47 | 141 | 373 | 433 | 468 | 498 | ---- |
| VM Stress Wndng (MPa)I | 521 | 680 | 687 | 581 | 469 | 487 | 459 | 689* |
| VM Stress Spprt (MPa)I | 732 | 918 | 907 | 1050 | 955 | 978 | 945 | ---- |
| Rad Intrfc Press (MPa) I | 123 | 168 | 170 | 173 | 82 | 72 | 63 | ---- |
| Rad Intrfc Press (MPa) F | 142 | 180 | 177 | 180 | 86 | 75 | 65 | ---- |
| VM Stress Wndng (MPa)F | 436 | 635 | 652 | 525 | 416 | 434 | 407 | ---- |
| VM Stress Spprt (MPa)F | 863 | 988 | 945 | 1095 | 987 | 1009 | 975 | ---- |
| VW Th Strs Wndng (MPa) I | 122 | 162 | 110 | 209 | 204 | 201 | 202 | ---- |
| VW Th Strs Shell (MPa) I | 190 | 262 | 116 | 165 | 116 | 113 | 108 | ---- |
| VW Th Strs Wndng (MPa) F | 205 | 207 | 146 | 268 | 263 | 259 | 260 | ---- |
| VW Th Strs Shell (MPa) F | 325 | 333 | 154 | 211 | 150 | 146 | 140 | ---- |
| | I= Flat Top Start, F= Flat Top End | | | | | * Overdrive to 20 T | | |

Table 2.

| Winding | one | two | three | four | five | six | seven | eight |
|---|---|---|---|---|---|---|---|---|
| Winding Effective Center Field (T) | 60 | 54.9 | 46.44 | 38.363 | 30.356 | 26.516 | 22.801 | 19.218 |
| Field Produced by Winding (T) | 5.1 | 8.46 | 8.077 | 8.007 | 3.84 | 3.715 | 3.583 | 19.218 |
| Alpha (Winding OD/Winding ID) | 1.53 | 1.64 | 1.33 | 1.20 | 1.07 | 1.06 | 1.05 | 1.68 |
| Beta (Winding Height/Winding ID) | 4.26 | 4.19 | 3.55 | 3.33 | 2.28 | 1.92 | 1.65 | 1.45 |
| Fraction of Max. Possible Field (%) | 95 | 95 | 95 | 95 | 92 | 88 | 84 | 74 |
| Winding ID (cm) | 4.75 | 9.06 | 18.3 | 30 | 43.8 | 52.16 | 60.52 | 69.08 |
| Winding OD (cm) | 7.26 | 14.9 | 24.4 | 36.1 | 46.86 | 55.22 | 63.58 | 116.32 |
| Winding Height (cm) | 20.25 | 38 | 65 | 100 | 100 | 100 | 100 | 100 |
| Winding Packing Factor | 0.65 | 0.70 | 0.70 | 0.70 | 0.70 | 0.70 | 0.70 | 0.74 |
| Conductor Size Hght x Wdth (cm) | .78x.47 | .95x.57 | 1.0x.6 | 1.0x.6 | 1.0x.6 | 1.0x.6 | 1.0x.6 | 1.4x1.0 |
| Conductor Cross-Sect. Area (cm^2) | 0.3613 | 0.5362 | 0.5947 | 0.5947 | 0.5947 | 0.5947 | 0.5947 | 1.3947 |
| Turns per Layer | 23 | 36 | 59 | 90 | 90 | 90 | 90 | 63 |
| Layers | 2 | 4 | 4 | 4 | 2 | 2 | 2 | 20 |
| Turns (total) | 46 | 144 | 236 | 360 | 180 | 180 | 180 | 1260 |
| Self Inductance (mH) | 0.0285 | 0.574 | 3.04 | 11.4 | 5.34 | 7.28 | 9.45 | 763 |
| Mutual Inductance w/ Winding 1 (mH) | | 0.0558 | 0.0566 | 0.0563 | 0.027 | 0.0261 | 0.0251 | 0.152 |
| Mutual Inductance w/ Winding 2 (mH) | | | 0.704 | 0.705 | 0.337 | 0.325 | 0.313 | 1.89 |
| Mutual Inductance w/ Winding 3 (mH) | | | | 3.57 | 1.69 | 1.63 | 1.56 | 9.41 |
| Mutual Inductance w/ Winding 4 (mH) | | | | | 5.71 | 5.46 | 5.24 | 31.8 |
| Mutual Inductance w/ Winding 5 (mH) | | | | | | 5.21 | 4.99 | 30.1 |
| Mutual Inductance w/ Winding 6 (mH) | | | | | | | 7.09 | 42.6 |
| Mutual Inductance w/ Winding 7 (mH) | | | | | | | | 57.5 |
| Resistance at Pulse Start (Ohms) | 0.0007 | 0.0051 | 0.0135 | 0.0315 | 0.0215 | 0.024 | 0.026 | 0.047 |
| Resistance at Pulse End (Ohms) | 0.0028 | 0.0128 | 0.0218 | 0.1085 | 0.074 | 0.0875 | 0.105 | 0.325 |
| Pulse Length (seconds) | 0.494 | 0.494 | 0.494 | 0.837 | 0.837 | 0.837 | 0.837 | 4.25 |
| Current Density in Cond. (kA/cm^2) | 51.6 | 34.76 | 31.34 | 31.34 | 31.34 | 31.34 | 31.34 | 11.85 |
| Current in a Turn (kA) | 18.64 | 18.64 | 18.64 | 18.64 | 18.64 | 18.64 | 18.64 | 16.52 |
| Peak Current in a Turn (kA) | 18.64 | 18.64 | 18.64 | 18.64 | 18.64 | 18.64 | 18.64 | 17.2 |
| Resistive Energy (MJ) | Windings 1, 2 & 3 = 2.63 | | | Windings 4, 5, 6 & 7 = 33.5 | | | | 123 |
| Peak Total Energy (MJ) | Windings 1, 2 & 3 = 3.7 | | | Windings 4, 5, 6 & 7 = 70 | | | | 290 |
| Peak Power (MW) | Windings 1, 2 & 3 = 19 | | | Windings 4, 5, 6 & 7 = 113 | | | | 168 |

Table 3.

## MAGNET SCHEDULE & COST ESTIMATE

| | TASK | TIME REQ'D | LATEST START | COST K$ |
|---|---|---|---|---|
| 1. | Material testing | 20 weeks | 1 FEB 93 | |
| 2. | Prototype testing | 30 weeks | 15 NOV 92 | 100 |
| 3. | Design & analysis | 26 weeks | 15 OCT 92 | |
| 4. | Prepare drawings | 8 weeks | 1 MAY 93 | |
| 5. | Obtain dewar fab. contract | 18 weeks | 1 DEC 93 | |
| 6. | Fab. dewar | 20 weeks | 1 APR 94 | 100 |
| 7. | Obtain cond. fab. contract | 16 weeks | 15 JUL 93 | |
| 8. | Fab. conductor | 18 weeks | 1 DEC 93 | 200 |
| 9. | Obtain shell fab. contract | 18 weeks | 1 JUL 93 | |
| 10. | Fab. shells | 20 weeks | 15 NOV 93 | 200 |
| 11. | Obtain coil fab. contract | 18 weeks | 1 DEC 93 | |
| 12. | Fab. coil | 20 weeks | 15 APR 94 | 200 |
| 13. | Obtain frame fab. contract | 18 weeks | 1 MAR 94 | |
| 14. | Fab. frame | 18 weeks | 1 JUN 94 | 100 |
| 15. | Install & test magnet | 12 weeks | 1 SEP 94 | |
| 16. | System commissioning | 18 weeks | 1 DEC 94 | |
| 17. | 60 T system ready | | 1APR 95 | |

Table 6.

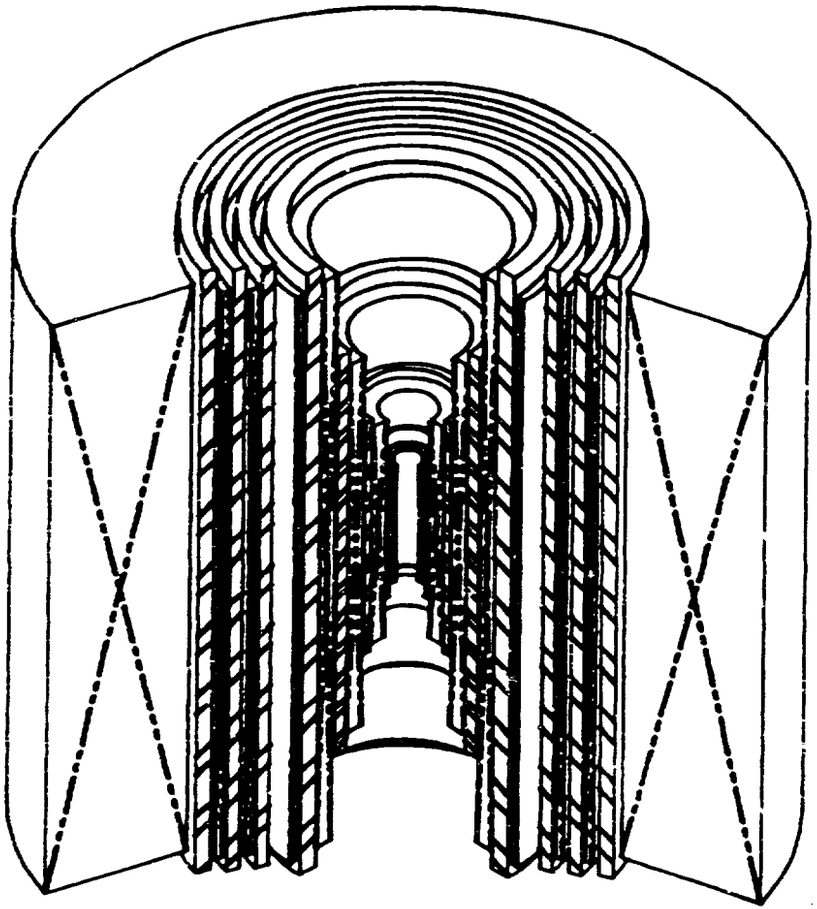

# 60 TESLA 100ms MAGNET WINDINGS & SHELLS

GROUP M6/LOS ALALMOS NATIONAL LABORATORY
NATIONAL HIGH MAGNETIC FIELD LABORATORY

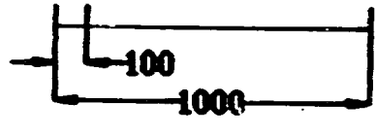


Dimensions are in MILLIMETERS
Dimensions in Brackets are in INCHES

Fig. 1

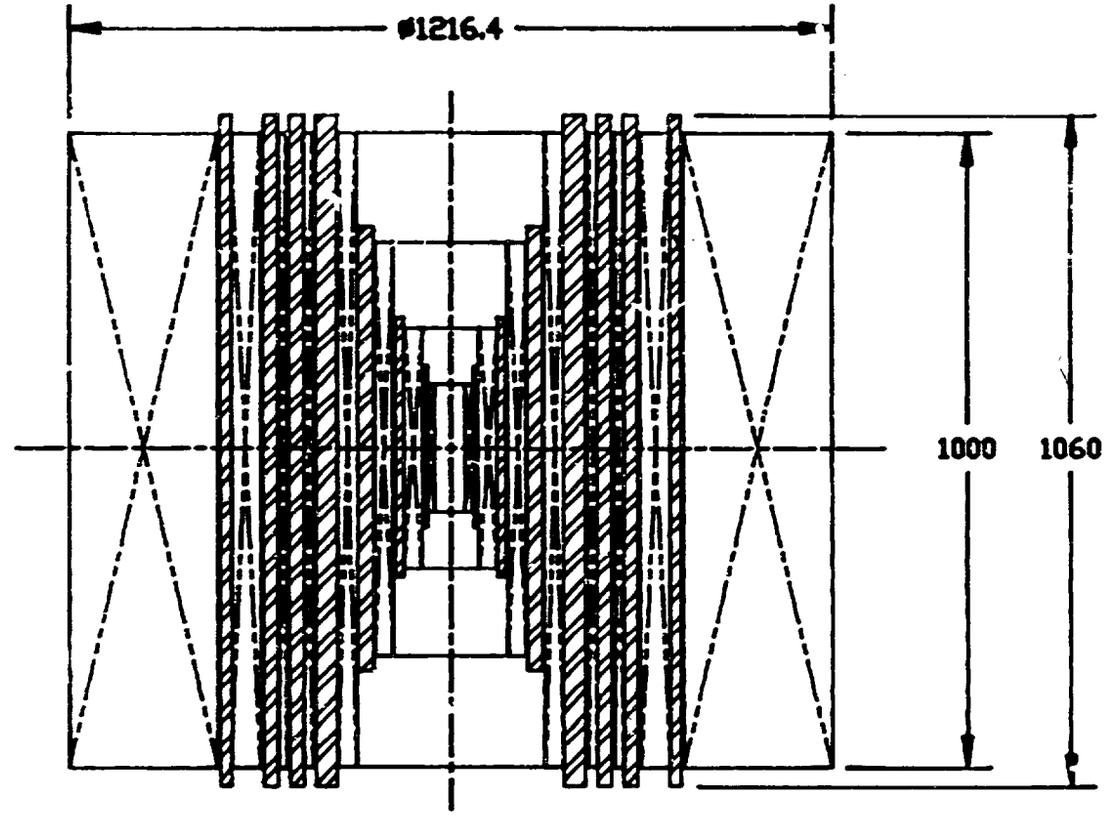


# 60 TESLA 100 ms MAGNET WINDINGS & SHELLS

GROUP M6/LOS ALAMOS NATIONAL LABORATORY
NATIONAL HIGH MAGNETIC FIELD LABORATORY

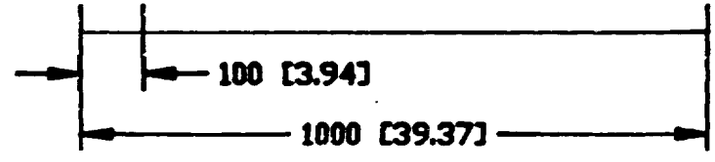


Dimensions are in MILLIMETERS
Dimensions in Brackets are in INCHES

Fig. 2

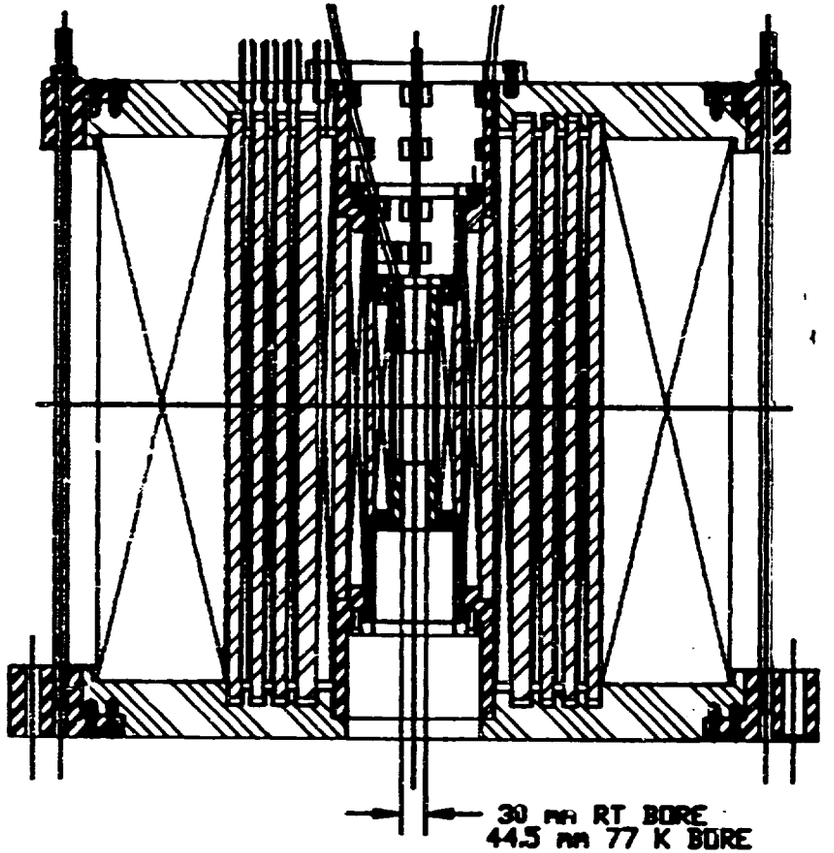


# 60 TESLA 100ms MAGNET

GROUP M6/LOS ALALMOS NATIONAL LABORATORY
NATIONAL HIGH MAGNETIC FIELD LABORATORY

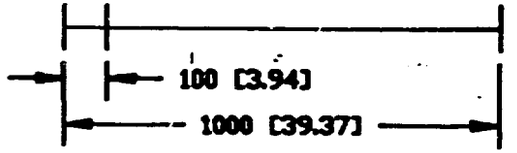


Dimensions are in MILLIMETERS
Dimensions in Brackets are in INCHES

Fig. 3

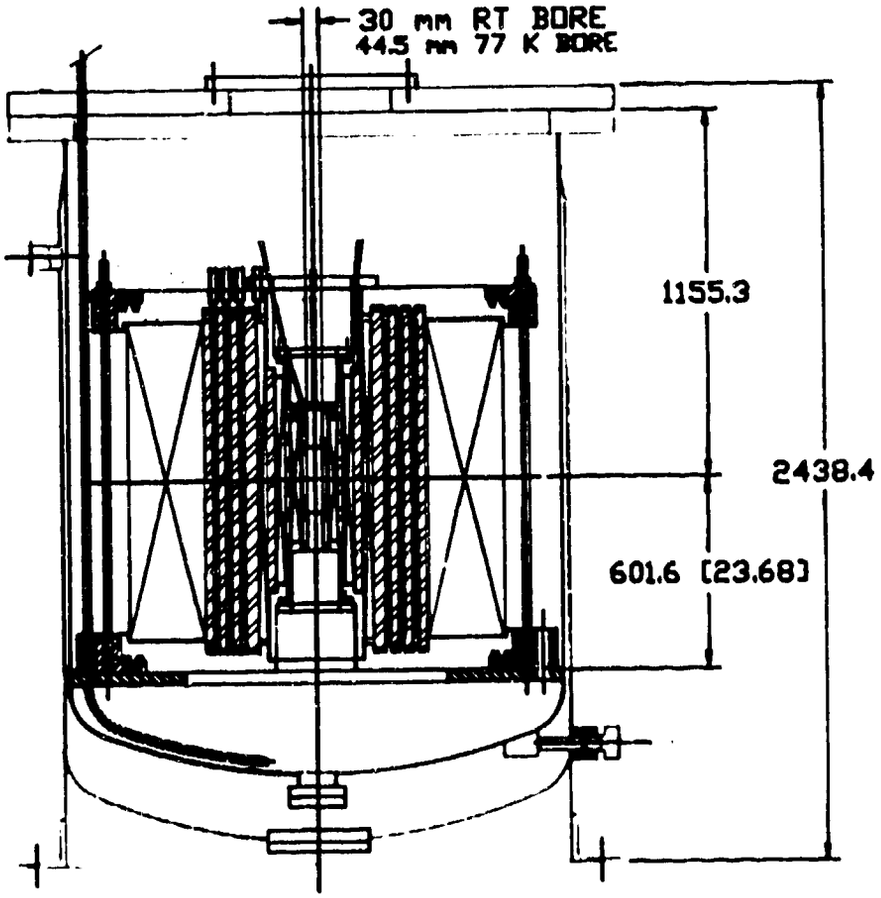


# 60 TESLA 100ms MAGNET & DEWAR

GROUP M6/LOS ALALMOS NATIONAL LABORATORY
NATIONAL HIGH MAGNETIC FIELD LABORATORY

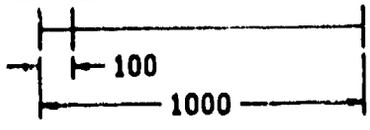


Dimensions are in MILLIMETERS
Dimensions in Brackets are in INCHES

Fig. 4

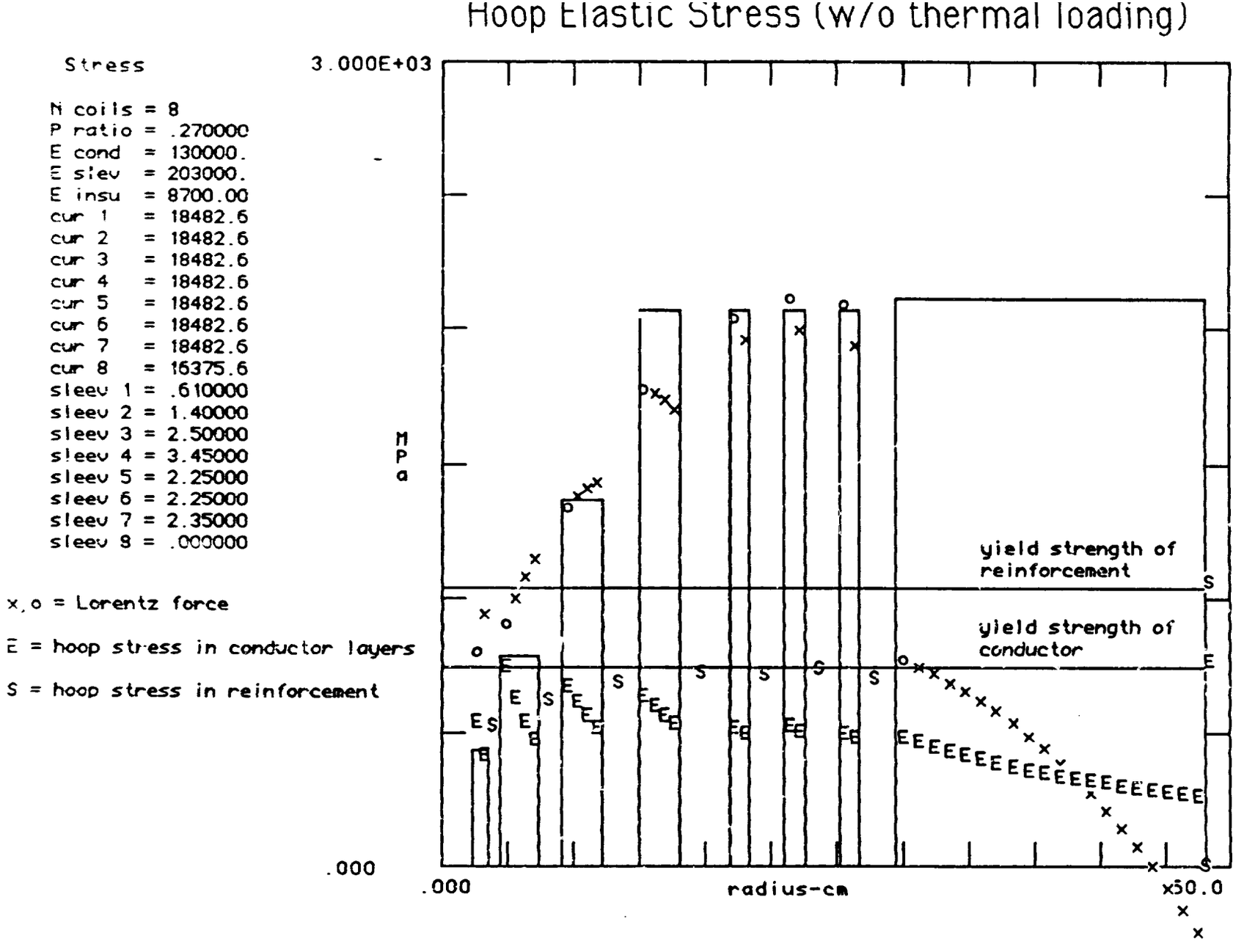
Hoop Elastic Stress (w/o thermal loading)
Stress
N coils = 8
P ratio = .270000
E cond = 130000.
E slev = 203000.
E insu = 8700.00
cur 1 = 18482.6
cur 2 = 18482.6
cur 3 = 18482.6
cur 4 = 18482.6
cur 5 = 18482.6
cur 6 = 18482.6
cur 7 = 18482.6
cur 8 = 16375.6
sleev 1 = .610000
sleev 2 = 1.40000
sleev 3 = 2.50000
sleev 4 = 3.45000
sleev 5 = 2.25000
sleev 6 = 2.25000
sleev 7 = 2.35000
sleev 8 = .000000
x,o = Lorentz force
E = hoop stress in conductor layers
S = hoop stress in reinforcement
3.000E+03
MPa
.000
.000
radius-cm
x50.0
yield strength of reinforcement
yield strength of conductor

Fig. 5

Displacement

| | |
|---|---|
| wr(1) | = .470000 |
| wz(1) | = .769000 |
| wr(end) | = 1.00000 |
| wz(end) | = 1.39500 |
| gap(i) = | |
| .3 3 3 4 .4 | |
| .4 .4 0 | |
| r1 1 | = 2.35000 |
| r1 2 | = 4.52000 |
| r1 3 | = 9.14000 |
| r1 4 | = 14.9800 |
| r1 5 | = 21.8700 |
| r1 6 | = 26.0400 |
| r1 7 | = 30.2100 |
| r1 8 | = 34.4800 |
| r2 1 | = 3.61000 |
| r2 2 | = 7.44000 |
| r2 3 | = 12.1800 |
| r2 4 | = 18.0200 |
| r2 5 | = 23.3900 |
| r2 6 | = 27.5600 |
| r2 7 | = 31.7300 |
| r2 8 | = 58.1200 |

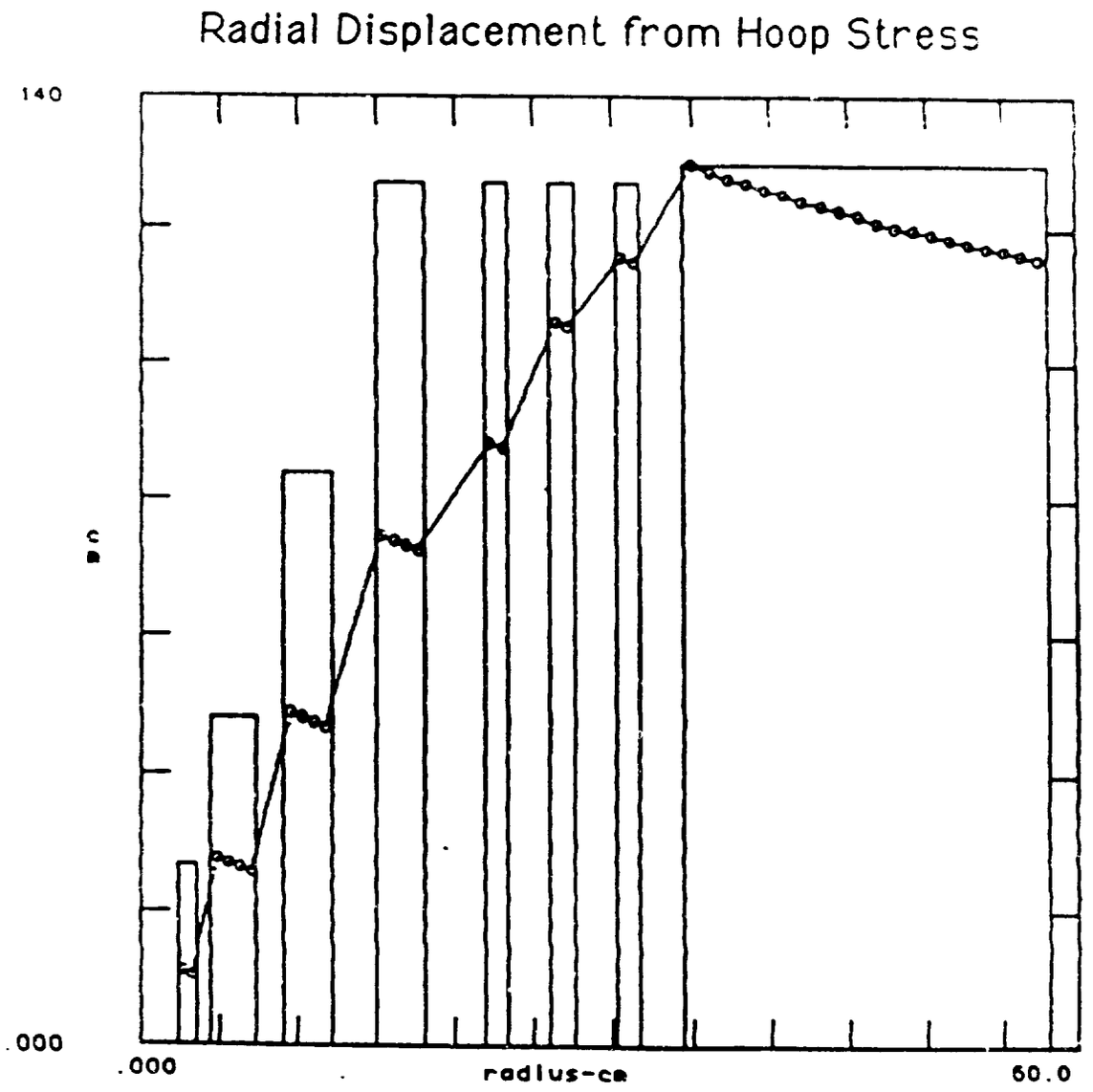


Fig 6

Elongation

% bore = 19.3416
wt. cond = 5.95717 ton
wt. sleu = .497680 ton
Σ layers= 40
Σ turns = 1306 x 2
layer 1 = 2
layer 2 = 4
layer 3 = 4
layer 4 = 4
layer 5 = 2
layer 6 = 2
layer 7 = 2
layer 8 = 20
turns 1 = 12 x 2
turns 2 = 18 x 2
turns 3 = 30 x 2
turns 4 = 45 x 2
turns 5 = 45 x 2
turns 6 = 45 x 2
turns 7 = 45 x 2
turns 8 = 32 x 2

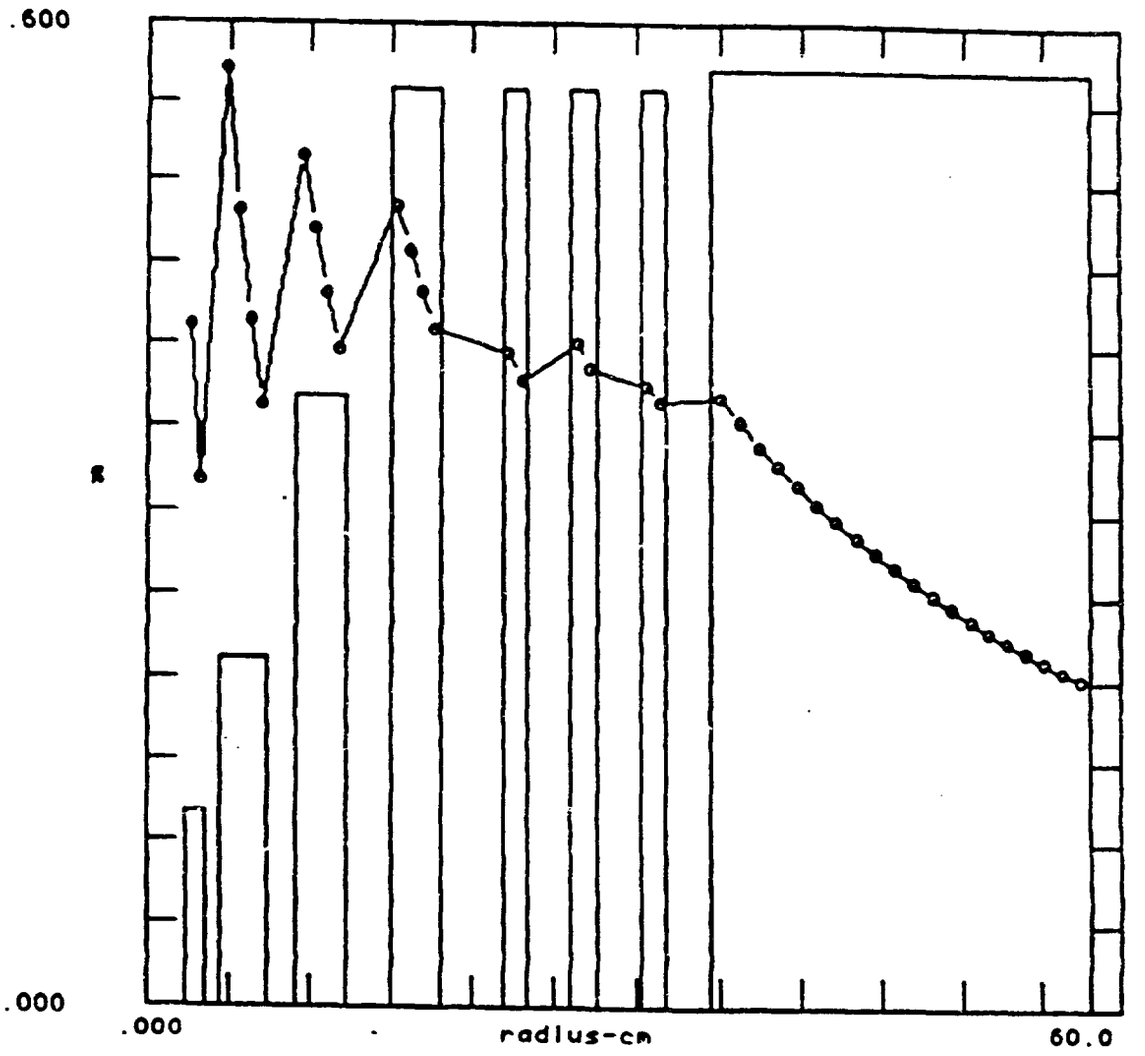


Fig 7

# Total Axial Stress at Midplane (w/o load sharing)

Axial Stress 450.

J 1 = 51.1375 Kamps/cm^2
J 2 = 34.4587 Kamps/cm^2
J 3 = 31.0841 Kamps/cm^2
J 4 = 31.0841 Kamps/cm^2
J 5 = 31.0841 Kamps/cm^2
J 6 = 31.0841 Kamps/cm^2
J 7 = 31.0841 Kamps/cm^2
J 8 = 11.7388 Kamps/cm^2

D = relative current density

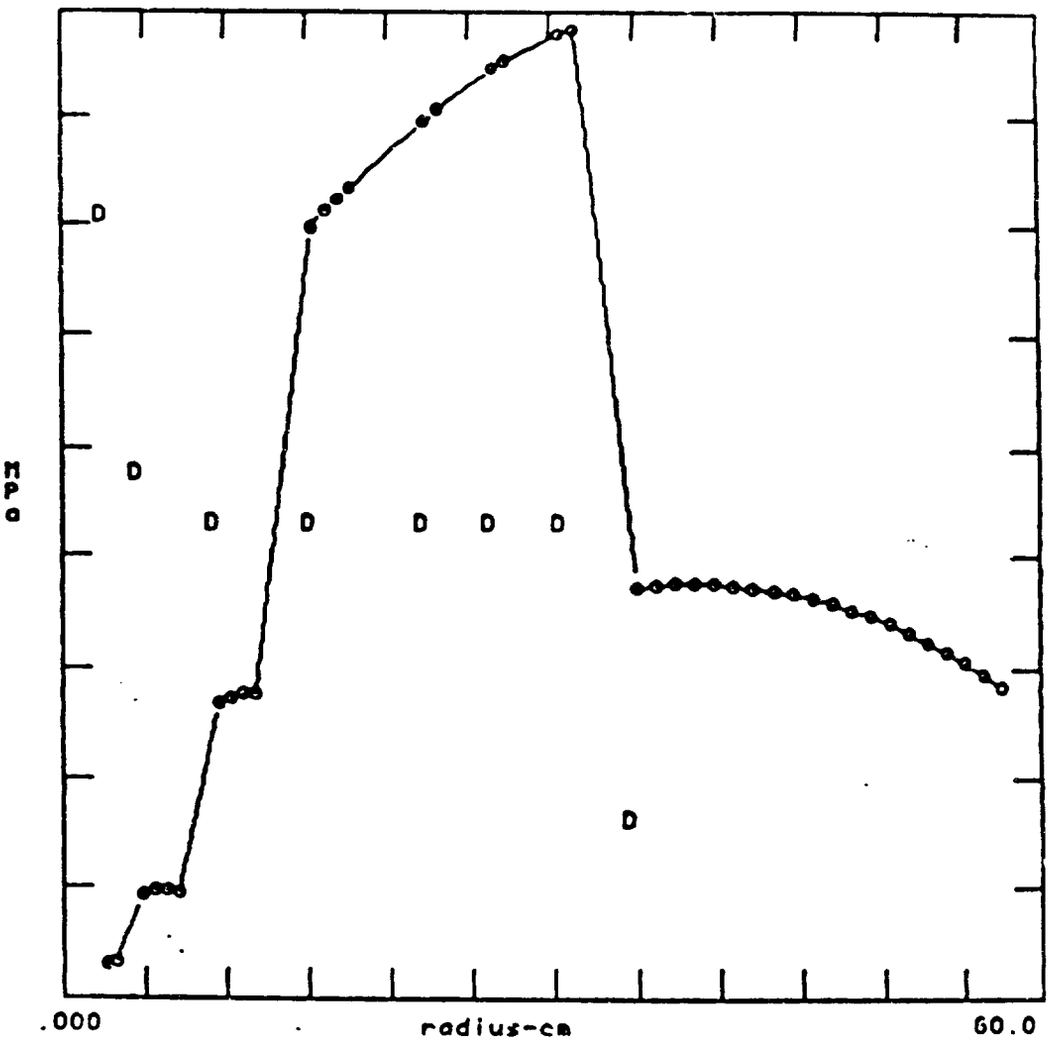


Fig. 8

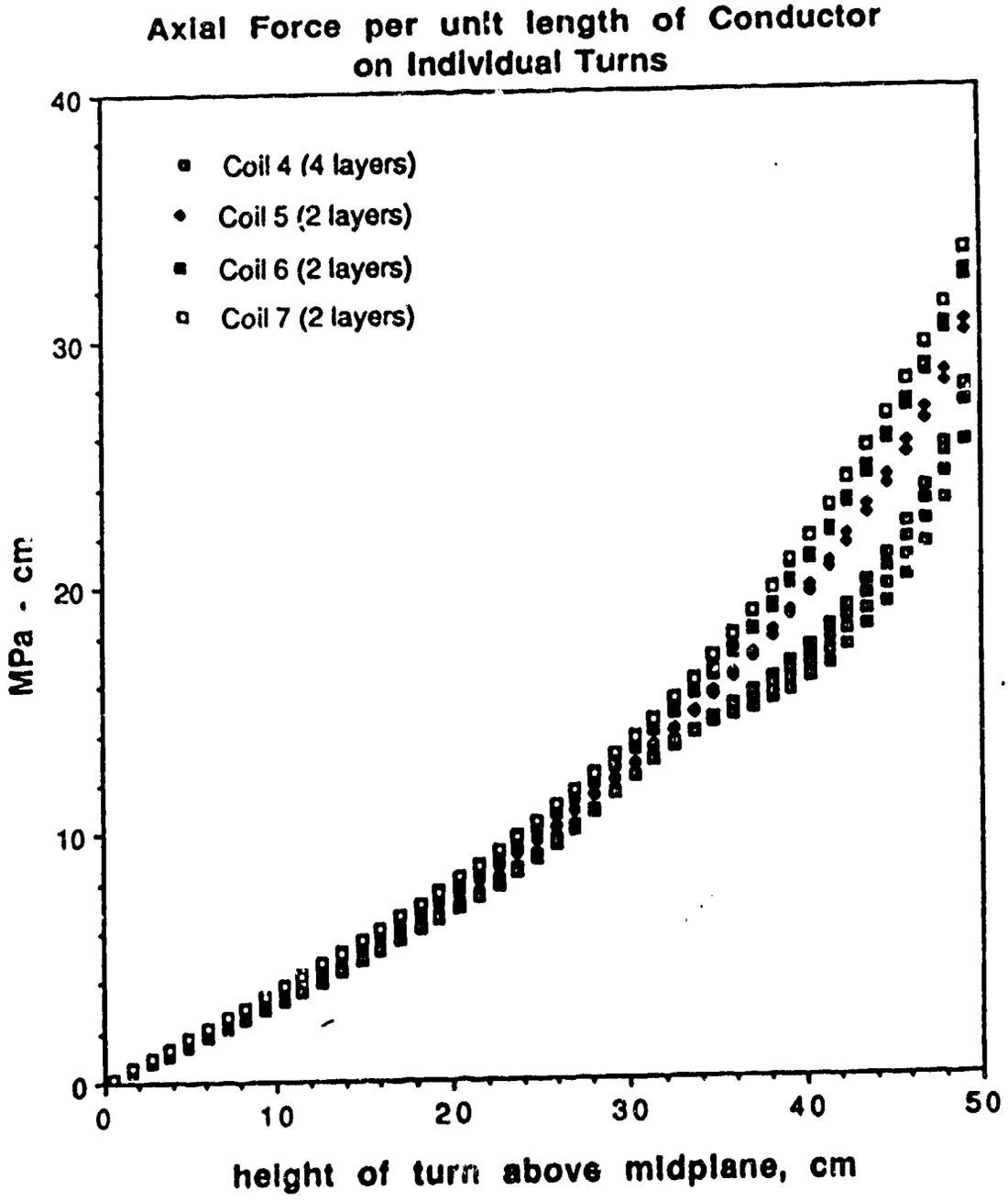
Axial Force per unit length of Conductor
on Individual Turns
Coil 4 (4 layers)
Coil 5 (2 layers)
Coil 6 (2 layers)
Coil 7 (2 layers)
MPa - cm
0
10
20
30
40
0
10
20
30
40
50
height of turn above midplane, cm

Fig. 9

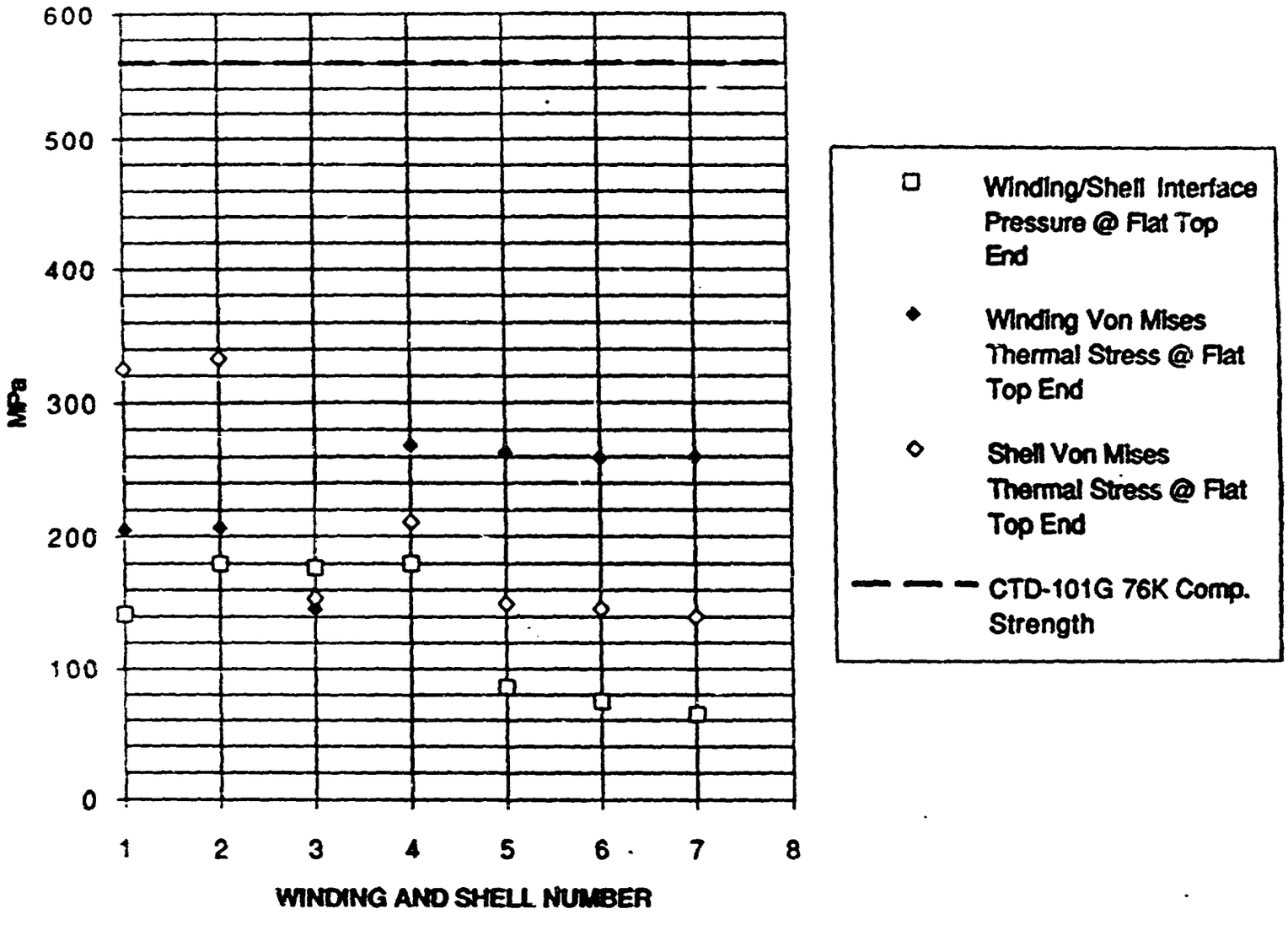
INTERFACE PRESSURE AND THERMAL STRESS
600
500
400
300
200
100
0
MPa
1
2
3
4
5
6
7
8
WINDING AND SHELL NUMBER
Winding/Shell Interface Pressure @ Flat Top End
Winding Von Mises Thermal Stress @ Flat Top End
Shell Von Mises Thermal Stress @ Flat Top End
CTD-101G 76K Comp. Strength

Fig. 10

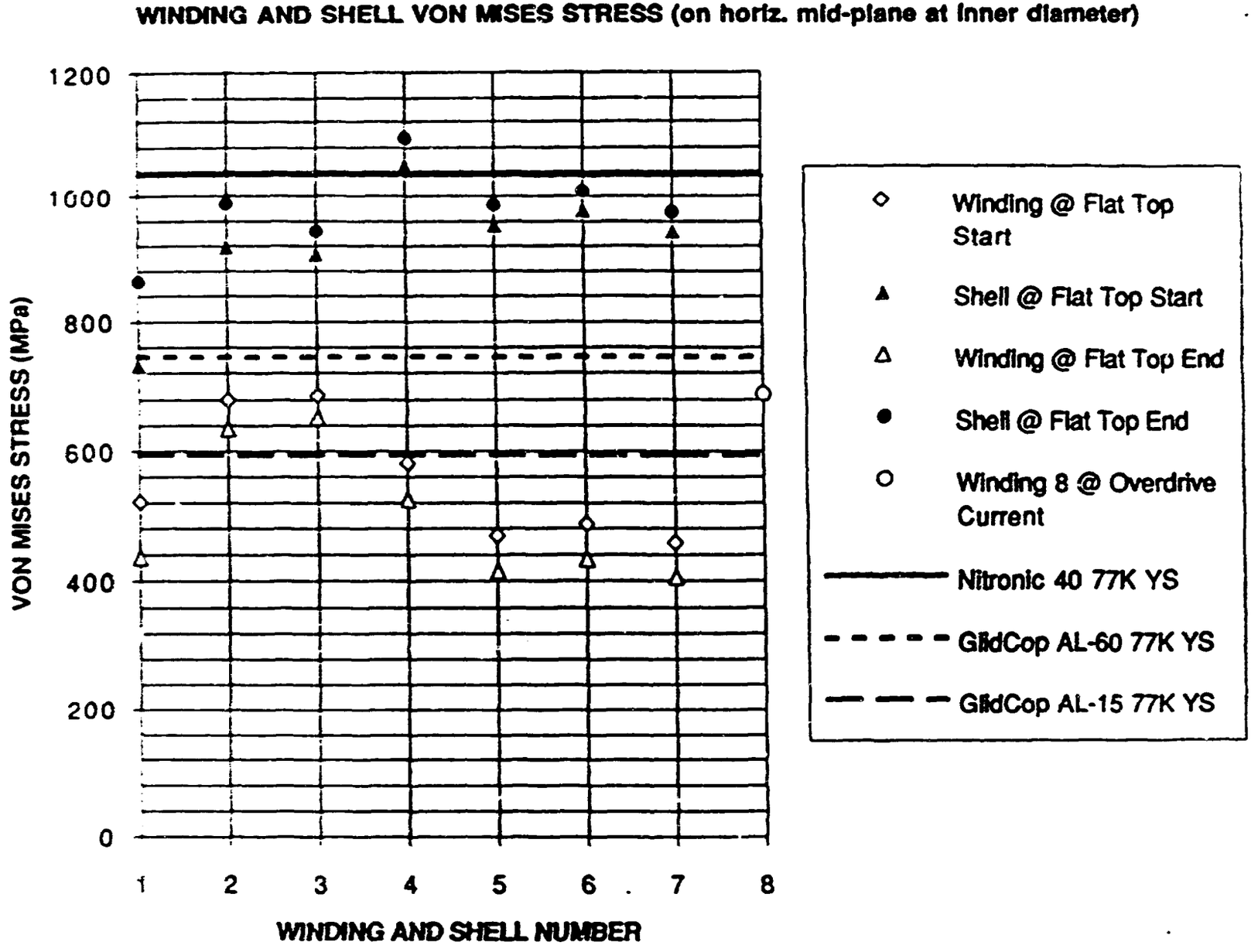
WINDING AND SHELL VON MISES STRESS (on horiz. mid-plane at inner diameter)
VON MISES STRESS (MPa)
1200
1000
800
600
400
200
0
1
2
3
4
5
6
7
8
WINDING AND SHELL NUMBER
Winding @ Flat Top Start
Shell @ Flat Top Start
Winding @ Flat Top End
Shell @ Flat Top End
Winding 8 @ Overdrive Current
Nitronic 40 77K YS
GlidCop AL-60 77K YS
GlidCop AL-15 77K YS

**Coil Lengths Compared to Saturation and Homogeneity Lengths**

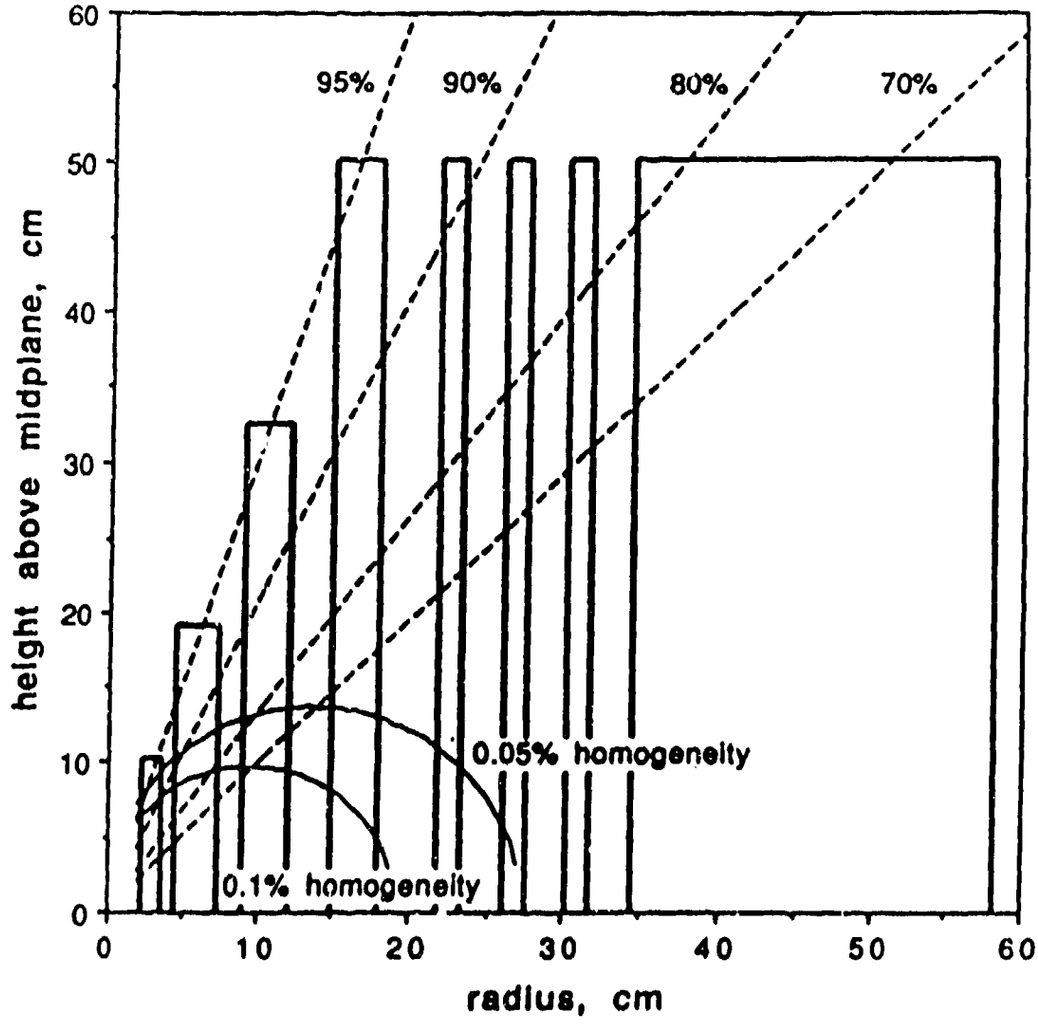


Fig 1.

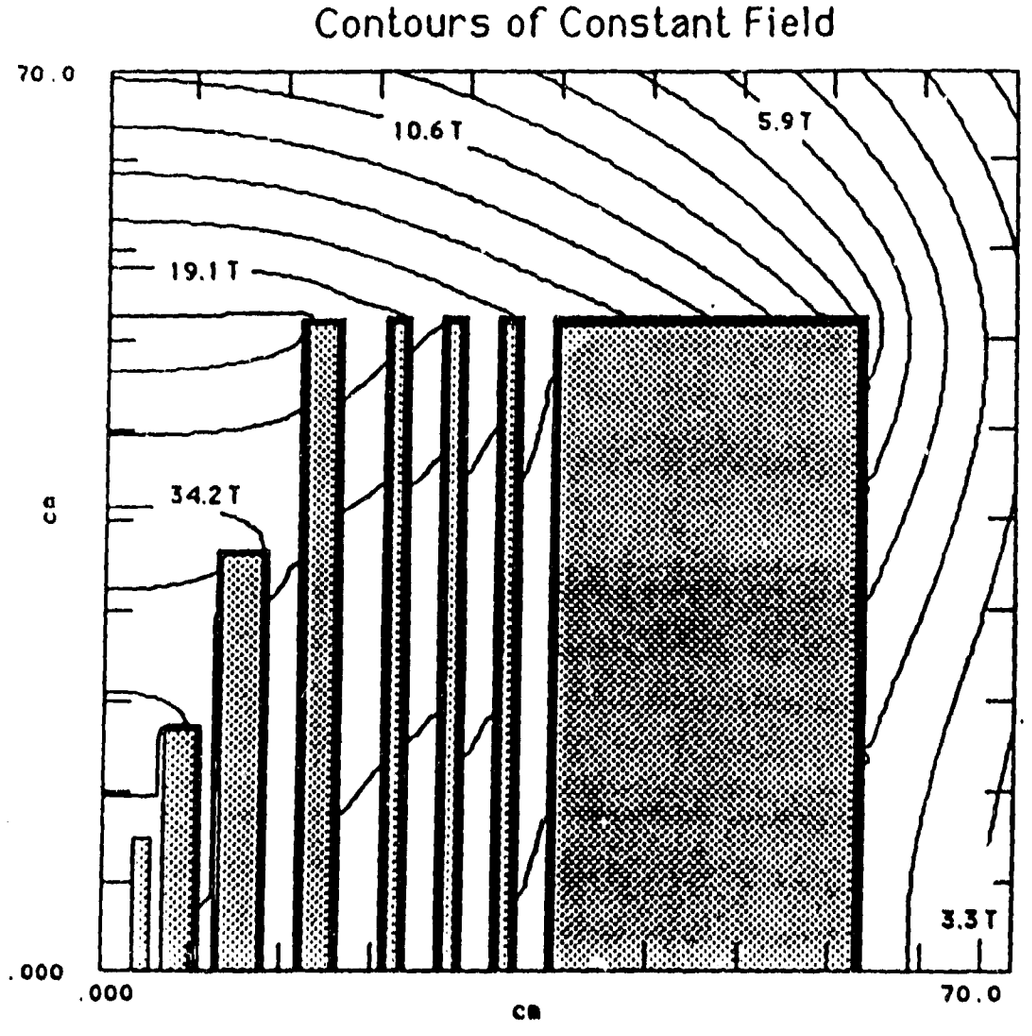
Contours of Constant Field
70.0
10.6 T
5.9 T
19.1 T
34.2 T
3.3 T
cm
.000
.000
70.0
cm

Bz

| | |
|---|---|
| r-cm | = 1.900000E-06 |
| pow MU | = 301.708 |
| Bz(0) | = 60.0000 tesla |
| B homog | = 1.222985E-04 |
| r sphr | = 1.00000 cm |
| Bz 1 | = 5.13833 |
| Bz 2 | = 8.45280 |
| Bz 3 | = 8.06179 |
| Bz 4 | = 7.99207 |
| Bz 5 | = 3.83192 |
| Bz 6 | = 3.70575 |
| Bz 7 | = 3.57298 |
| Bz 8 | = 19.2244 |
| power 1 | = 1.613963E+06 |
| power 2 | = 6.547257E+06 |
| power 3 | = 1.754704E+07 |
| power 4 | = 4.074007E+07 |
| power 5 | = 2.793781E+07 |
| power 6 | = 3.308587E+07 |
| power 7 | = 3.823394E+07 |
| power 8 | = 1.360017E+08 |

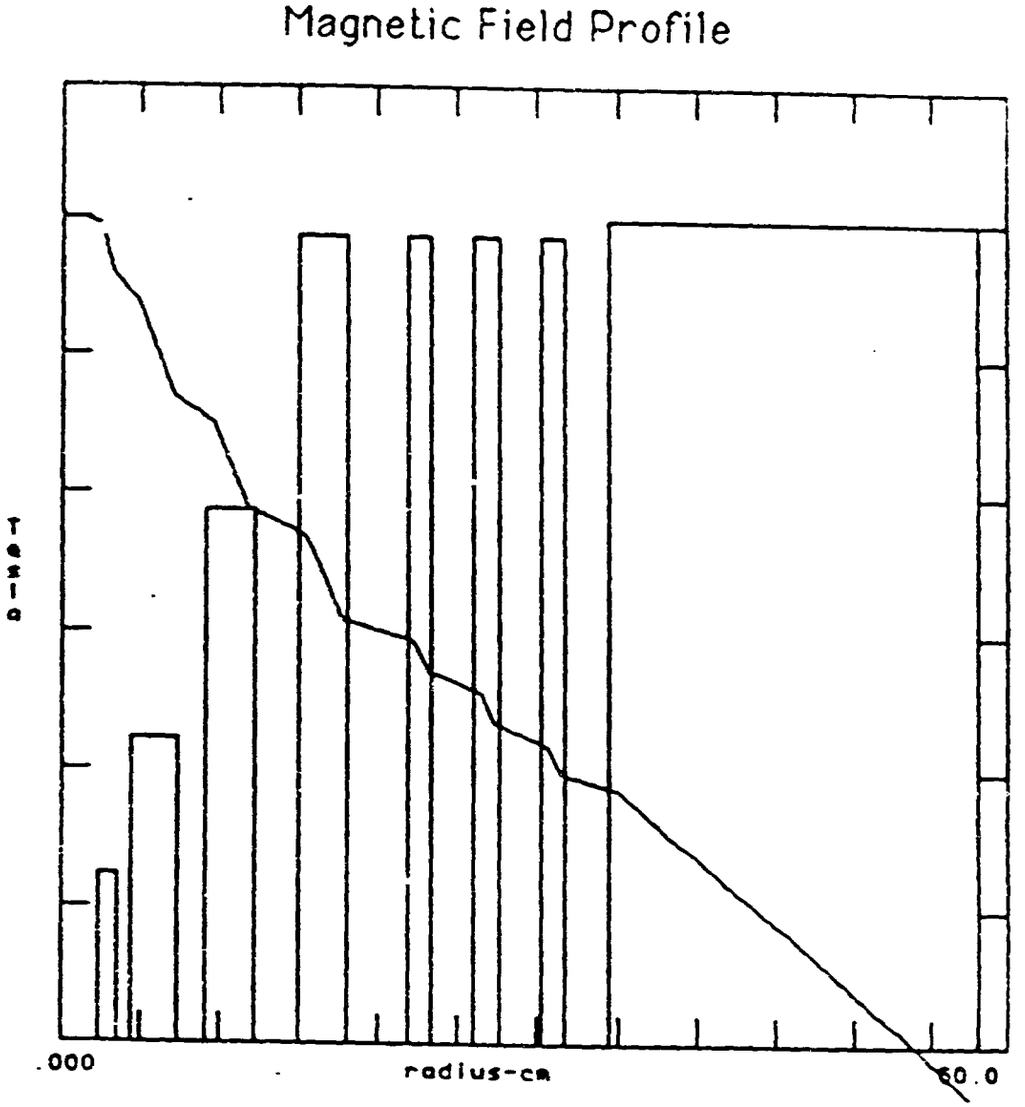

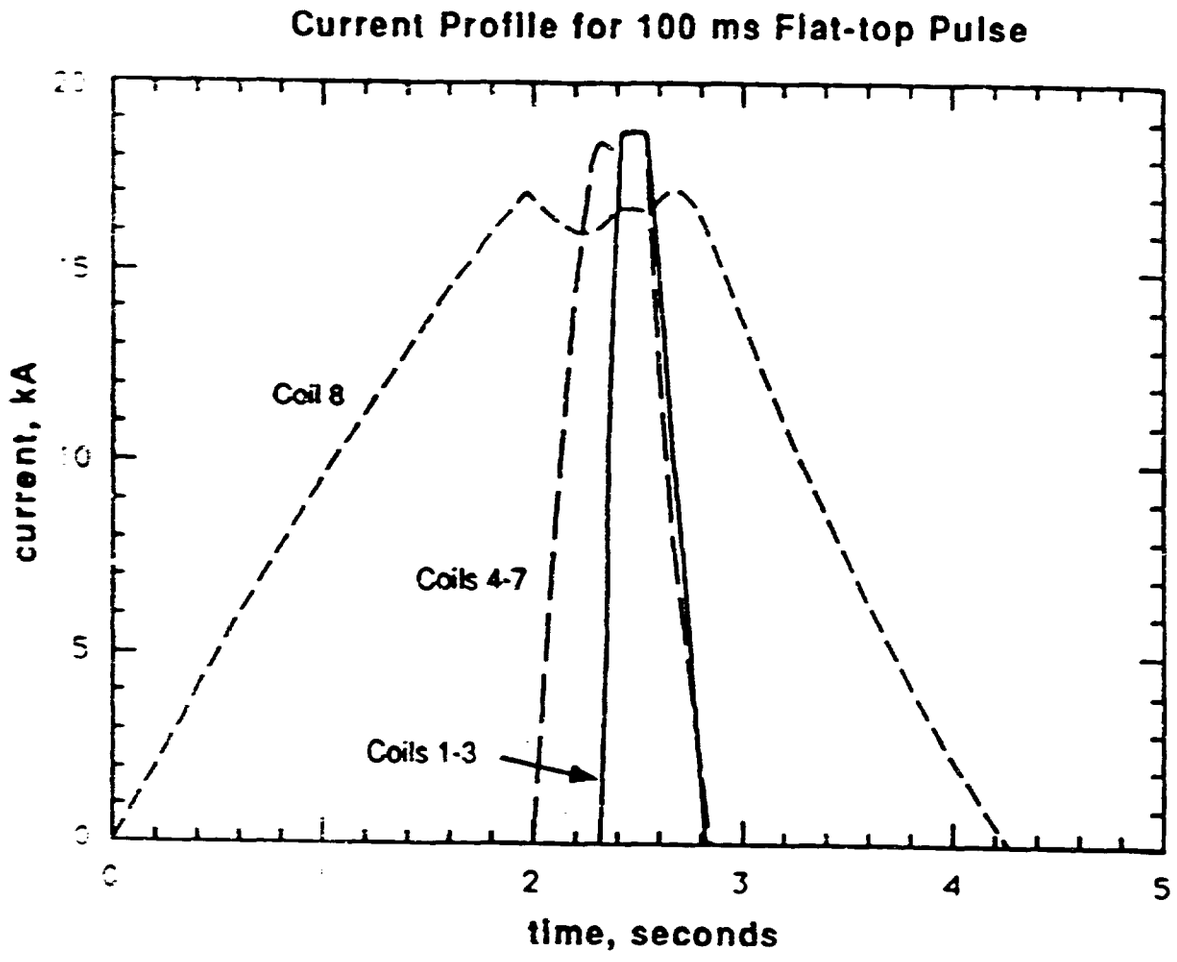
Current Profile for 100 ms Flat-top Pulse
current, kA
time, seconds
Coil 8
Coils 4-7
Coils 1-3
0
5
10
15
20
0
2
3
4
5

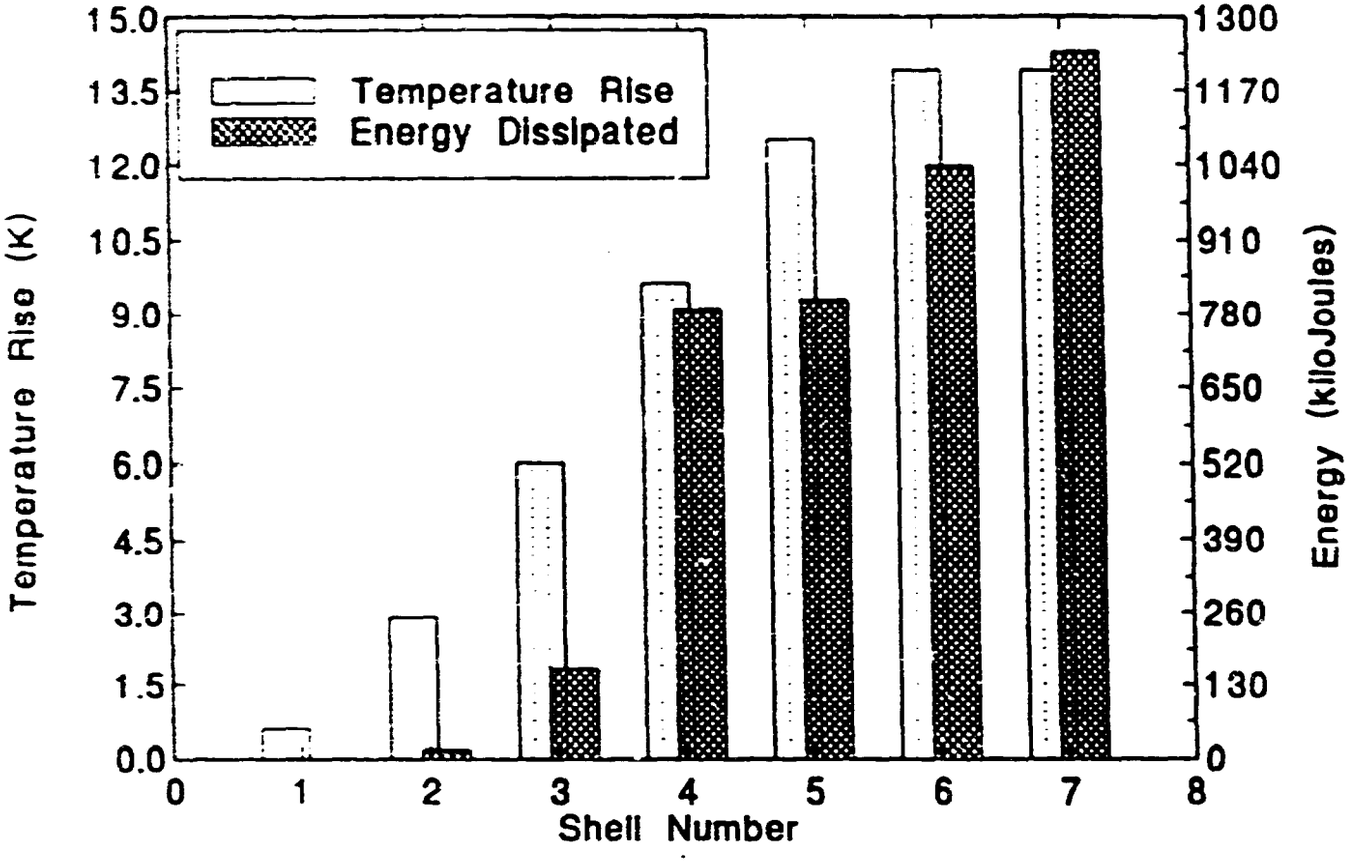
Temperature Rise
Energy Dissipated
Temperature Rise (K)
Energy (kiloJoules)
Shell Number
15.0
13.5
12.0
10.5
9.0
7.5
6.0
4.5
3.0
1.5
0.0
1300
1170
1040
910
780
650
520
390
260
130
0
0
1
2
3
4
5
6
7
8

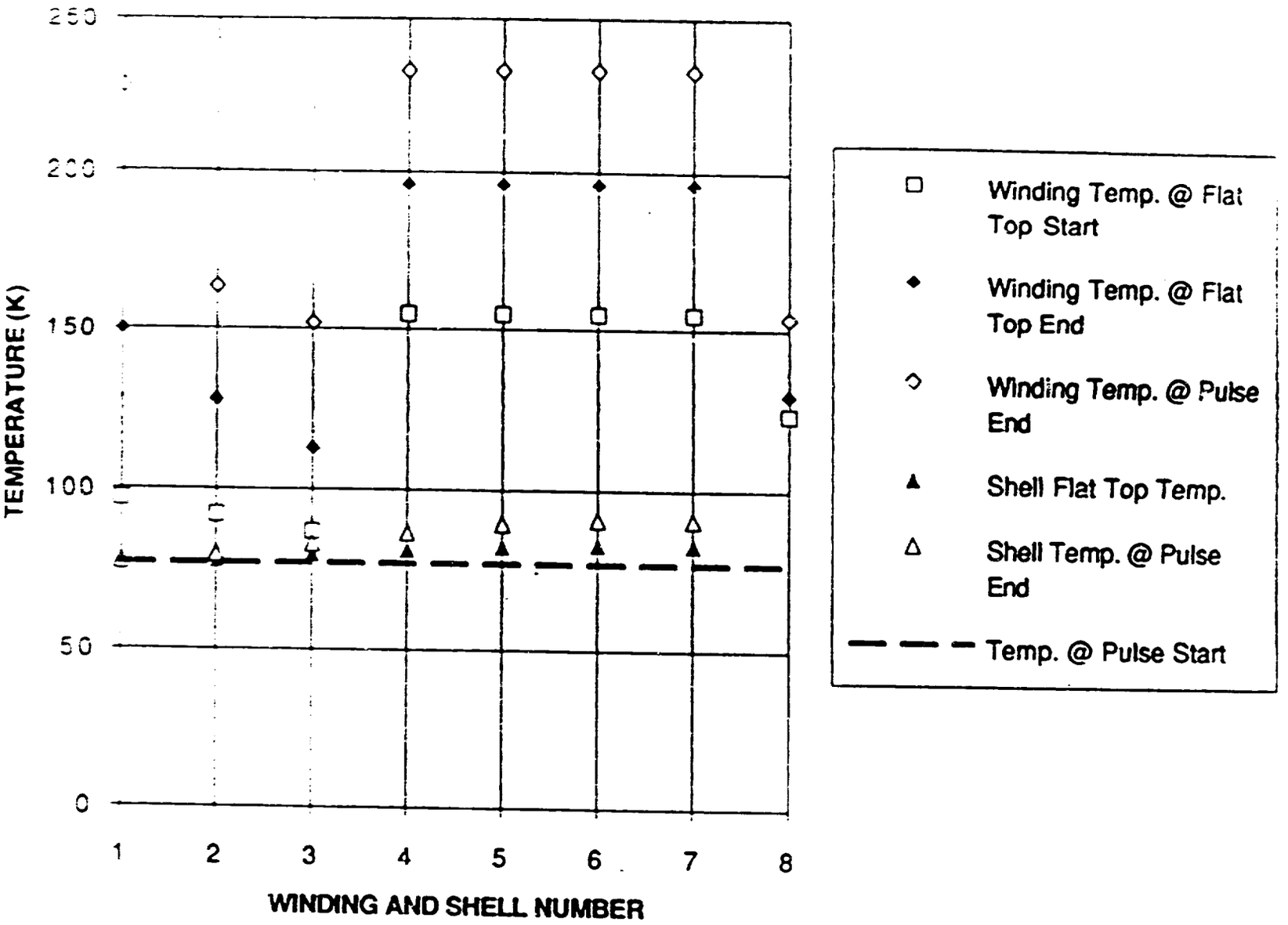
WINDING AND SHELL TEMPERATURE
250
200
150
100
50
0
TEMPERATURE (K)
1
2
3
4
5
6
7
8
WINDING AND SHELL NUMBER
Winding Temp. @ Flat Top Start
Winding Temp. @ Flat Top End
Winding Temp. @ Pulse End
Shell Flat Top Temp.
Shell Temp. @ Pulse End
Temp. @ Pulse Start

Fig 18

## OUTER COIL COOL-DOWN

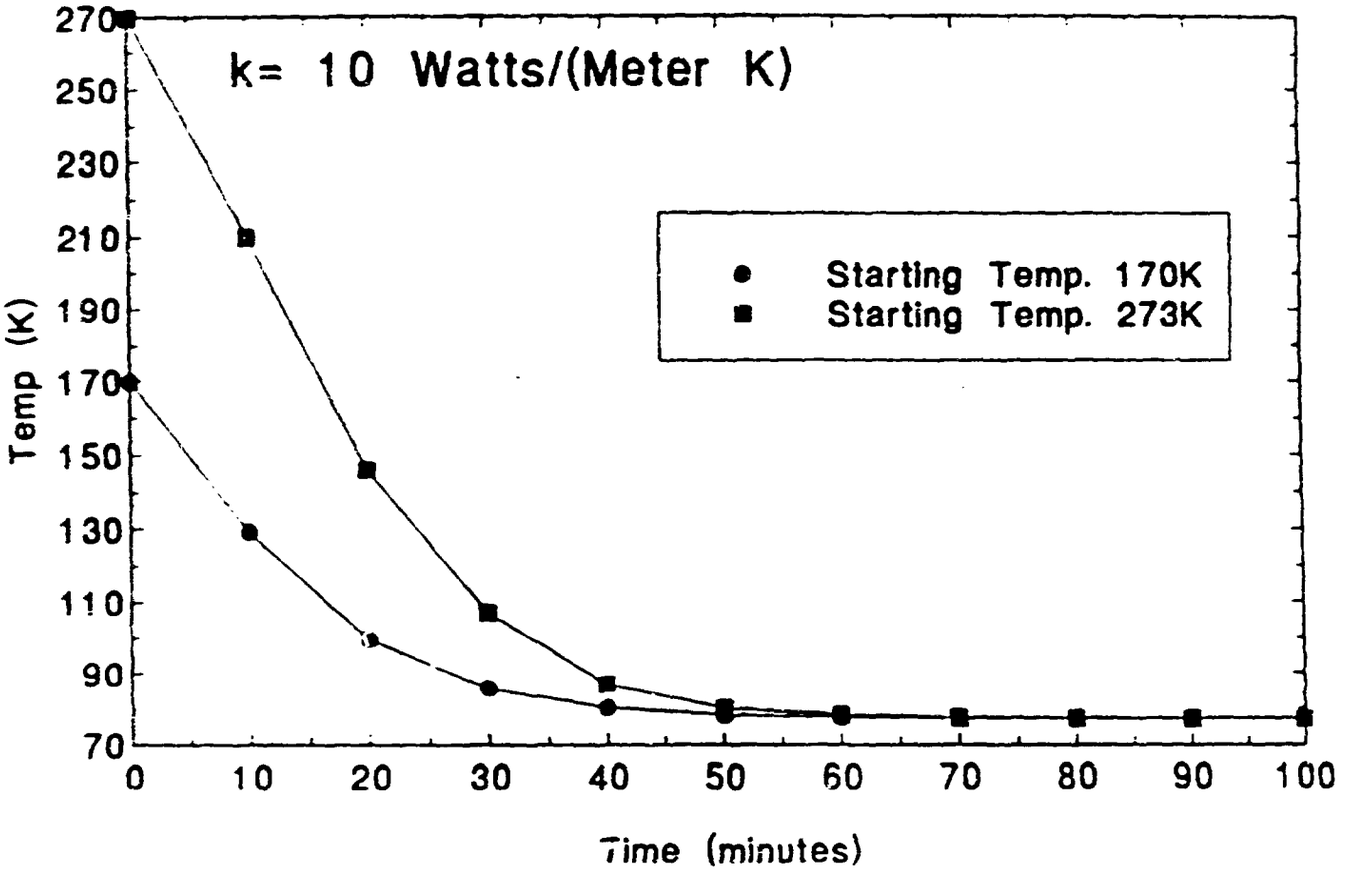

# OUTER COIL COOL-DOWN

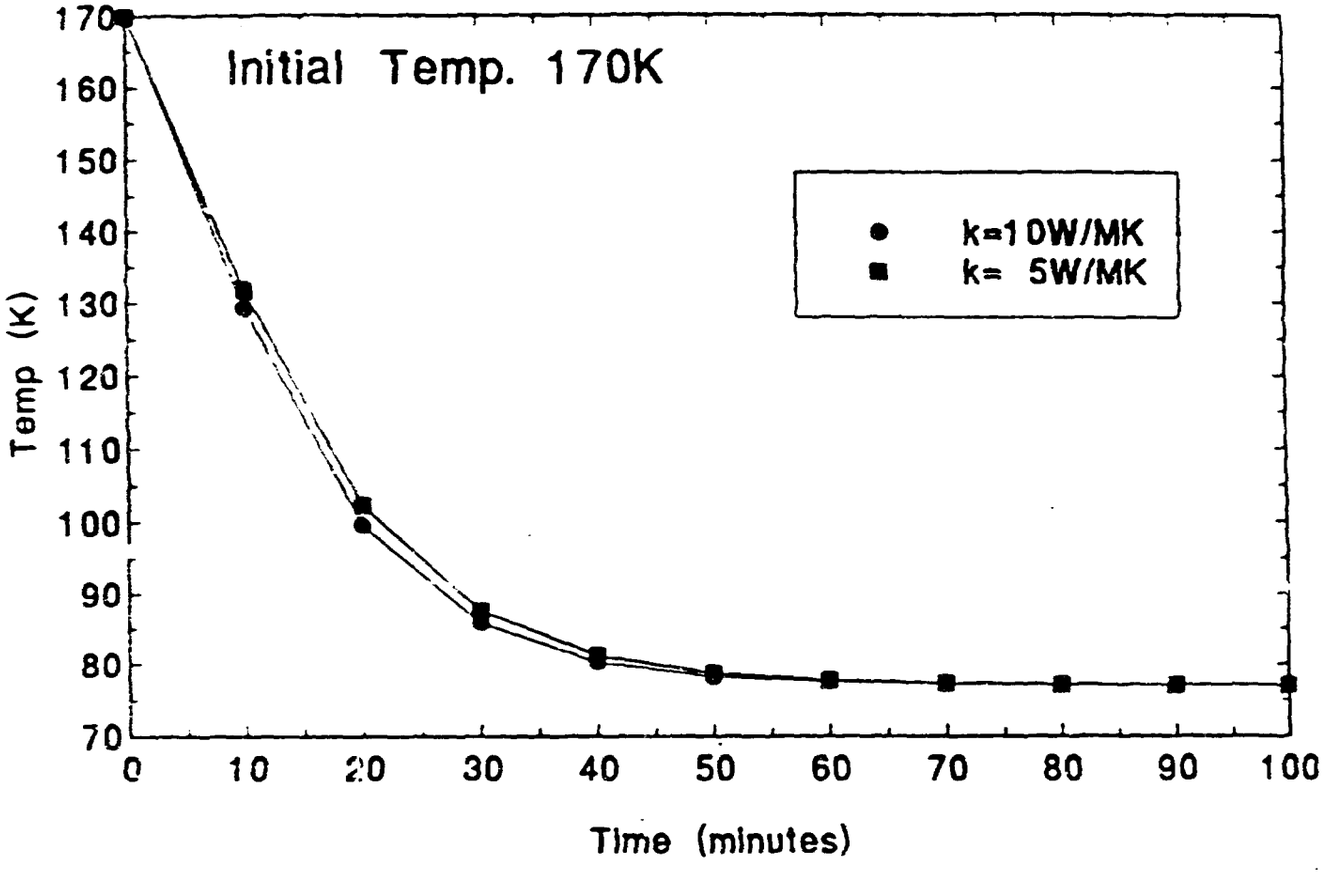

# COIL COOL-DOWN